universität wien

MASTERARBEIT

"Pathogenicity of $AQP4_{207-232}$ specific T-cells and the contribution of neutrophils to lesion formation"

verfasst von

Bleranda Zeka, BSc

angestrebter akademischer Grad

Master of Science (MSc)

Wien, 2014

Studienkennzahl lt. Studienblatt:	A 066 834
Studienrichtung lt. Studienblatt:	Masterstudium Molekulare Biologie
Betreut von:	Assoc. Prof. Dr. Monika Bradl

Inhalt

1. Zusammenfassung

Neuromyelitis optica (NMO) ist eine entzündliche, entmarkende Erkrankung des zentralen Nervensystems. Die Entdeckung eines Antikörpers, der sich gegen den Wasserkanal Aquaporin-4 (AQP4), richtet, ermöglichte die Identifizierung wichtiger Krankheitsmechanismen, wie die Interaktion dieses Antikörpers mit AQP4 auf Astrozyten, die Fixierung von Komplement durch diesen Antikörper und die daraus resultierende Rekrutierung von Effektorzellen ins Gewebe. Die Frage, auf welchem Weg diese die Bluthirnschranke passieren, ist noch nicht geklärt. Im Tiermodel wurde gezeigt, dass ZNS-spezifische T-Zellen die Bluthirnschranke überqueren können und Komplement, sowie Effektorzellen an den Entzündungsherd rekrutieren können.

In vorangehenden Studien untersuchten wir welche spezifischen AQP4 Motive über den MHC-Klasse-II-Weg in Lewis Ratten präsentiert werden können. Eines zeigte das höchste pathogene Potential. Hervorrufen einer EAE (Experimentelle autoimmune Enzephalomyelitis) durch aktivierte T-Zellen hat bisher zu den meisten Lesionen geführt. Diese T-Zellen können allerdings nicht in das Parenchym einwandern.

Um dieser Dominanz von Loop E-spezifischen T-Zellen auf den Grund zugehen, haben wir die Expression einer speziellen AQP4-Isoform, die nicht für Loop E kodiert (AQP4Δ4), im Thymus von Lewis Ratten untersucht. Eine solche Expression könnte es T-Zellen ermöglichen der negativen Selektion im Thymus zu entgehen. Wir konnten allerdings die bereits beschriebene Expression von AQP4Δ4 in Muskelgeweben nicht verifizieren und konnten auch keine Expression von AQP4Δ4 im Thymus nachweisen. Als weiteren Teil, haben wir den Einfluss von einer erhöhten Anzahl an Neutrophilen im Blut auf die Pathogenität von Loop E spezifischen T-Zellen untersucht. Zusätzlich zeigen wir, dass eine erhöhte Neutrophilen-Anzahl nicht zur Infiltration von T-Zellen und Effektorzellen ins Parenchym führt.

2. Abstract

The discovery of antibodies against the water channel aquaporin-4 (AQP4), which is mainly expressed on astrocytes has enabled researchers to identify key immunological players in neuromyelitis optica (NMO). However, it remains an open question how these pass the Blood-Brain-Barrier (BBB). In animal models it has been shown that CNS-antigen specific T-cells pass the BBB and recruit antibodies, complement and effector cells but identifying

AQP4 peptide specific T-cells which induce a disease with neurological symptoms has been a challenge. Previous studies from our lab investigated the specific peptide-binding motifs for MHC class II molecules of the Lewis rat. Of all 9 predicted AQP4 epitopes so far one epitope has shown the highest pathogenic potential, which resides in loop E. EAE (experimental autoimmune encephalomyelitis) mediated by loop E-specific T-cells results in the highest number of inflammatory lesions in the CNS, but the T-cells do not infiltrate the parenchyma. In order to explain this dominance we investigated the presence of an isoform of AQP4 which lacks loop E (AQP4Δ4) in the thymus of Lewis rats. This may allow loop E-specific T-cells to escape negative selection in the thymus. Additionally, we investigated whether increasing the neutrophil count increases the pathogenicity of loop E-specific T-cells. We could not detect AQP4Δ4 in the thymus. Additionally, we show that the elevation of the number of neutrophils does not lead to infiltration of T-cells and effector cells into the parenchyma. The reasons for the low pathogenic potential of AQP4 peptide specific T-cells have yet to be elucidated.

3. Introduction

Neuromyelits Optica (NMO, Devic's disease) is an inflammatory demyelinating disease of the central nervous system characterized by uni- or bilateral optic neuritis and acute myelitis. Despite the different disease pathology, NMO has long been classified a subtype of Multiple Sclerosis (MS) but with the discovery of a disease-associated antibody (NMO-IgG) NMO is universally considered a distinct disease (Wingerchuk et al., 2006a).

Although cases of optic neuritis and myelitis had been reported from different countries before, it was Eugine Devic and his student in 1894 who described similar clinical features in different cases and recognized those as characteristics of a distinct disease which they termed "neuromyelits optica" (Fujihara et al., 2012). Since then there has been a lot of confusion regarding the definition and characteristics of NMO. In this work Devic analyzed data from patients suffering from monophasic and relapsing NMO, as well as cases showing symptoms in the brain. Regardless, some subsequent reports only consider monophasic cases as NMO (Wingerchuk et al., 2006b), as well as required the absence of brain symptoms (Wingerchuk et al., 2006a). In Japan, where MS was reported very rarely until the 1960s (Kira, 2003), Patients with relapsing NMO were diagnosed with optic-spinal Multiple

Sclerosis (OSMS) (Misu et al., 2002). Generally, speaking of NMO as a separate disease rather than a subtype of MS was controversial. Some researchers continued to define NMO as a severe variant of MS even after the discovery of NMO-IgG (Lennon et al., 2005).

Soon after NMO-IgG had been linked to NMO, the antibody was found to bind astrocytic end feet next to the microvasculature, the Virchow-Robin spaces and the pia mater, with the exact target being the most abundant water channel in the CNS, aquaporin-4 (AQP4). This provided for a whole new range of research perspectives for NMO pathology, diagnosis and treatment (V. a Lennon et al., 2005; V. A. Lennon et al., 2004).

3.1. Symptoms and Diagnosis

NMO begins with uni- or bilateral optic neuritis and longitudinally extensive transverse myelitis, a continuous MRI lesion extending over three or more vertebral segments. Brain lesions are not part of the onset symptoms, but most NMO patients do develop brain lesions as the disease progresses (Wingerchuk et al., 2006b). Other symptoms either arise from the optic neuritis, like ocular pain, visual field deficits and positive phenomena, or from the myelitis, like bilateral motor weakness, sensory level sphincter and bladder dysfunction. In case of brainstem involvement, this may cause hiccups, intractable nausea and vomiting, or respiratory failure. Evidently, demyelination of the spinal cord causes typical symptoms, like paroxysmal spasms, which are recurrent painful spasms of the limbs and trunk, and Lhermitte's symptom, which is a spinal or limb dysaesthesia caused by neck flexion (Jacob et al., 2007; Wingerchuk et al., 2007).

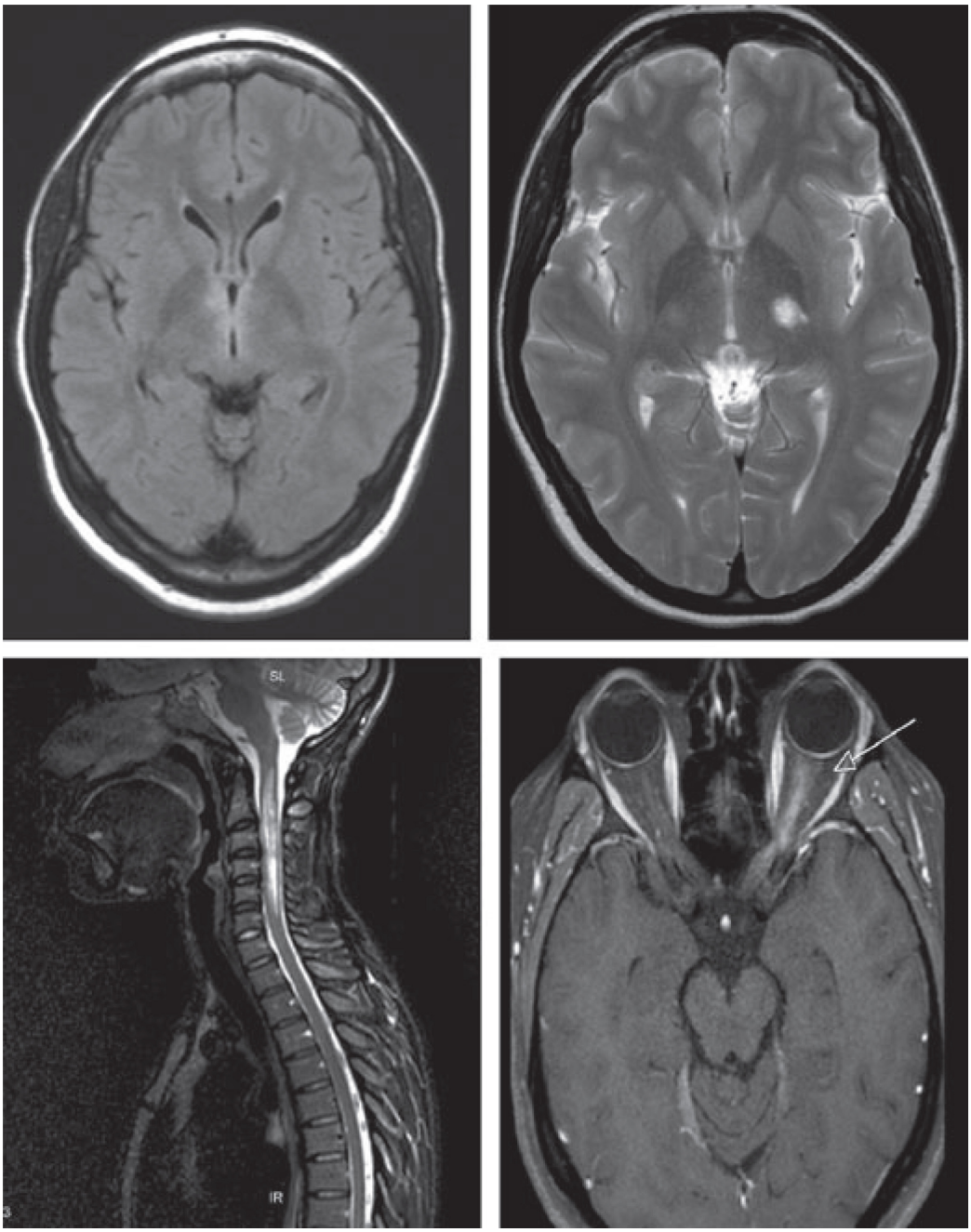

Figure 1: Central nervous system lesions typical of neuromyelitis optica (NMO). Representative magnetic resonance imaging (MRI) of patients with NMO seropositive for anti-aquaporin4 antibodies⁄ NMO -IgG, from the authors_ clinic. (A) Fluid-attenuated inversion recovery (FLAIR) shows signal abnormality around the third ventricle. (B) T2-weighted MRI signal abnormality in the thalamus and posterior limb of internal capsule on the left side. (C) Sagittal T2-weighted MRI of cervical spinal cord from a patient with NMO, showing longitudinally extensive transverse myelitis with swelling. (D) Gadolinium enhancement T1-weighted image shows optic neuritis on the left side. Figure and legend (Asgari et al., 2011). Copyright 2010 with permission John Wiley & Sons A/S

NMO can be monophasic or relapsing. Patients who suffer from monophasic NMO will not experience any remission after disease onset. Most patients, however, will go through remission phases after relapses. Nonetheless, the recovery is often incomplete and the relapses worsen (Argyriou and Makris, 2008). There are more differences between

monophasic and relapsing disease course, relapsing NMO has a female prevalence, the disease sets on at older age and is often associated with autoimmune disease background (Fujihara et al., 2012; Wingerchuk et al., 2006b). Those systemic autoimmune diseases can be organ-specific including thyroid disease, type 1 diabetes, celiac disease and myasthenia gravis (Jacob et al., 2013) or non-organ-specific like systemic lupus erythematsus and Sjögren's syndrome (Pittock et al., 2008).

However, both monophasic and relapsing NMO can be associated with NMO-IgG seropositivity, albeit not very often in monophasic NMO patients (Jarius and Wildemann, 2013; Ketelslegers et al., 2011).

In effect, although the symptoms are not particularly diverse, diagnosing patients with NMO has been a challenge for many doctors in the past. This is mainly due to the similarity to MS, the controversy about the autonomy of NMO, the occasional coexistence of another autoimmune disease, and later, due to the absence of NMO-IgG in some patients. In order to diagnose NMO, Wingerchuk's "Revised Diagnostic Criteria for Neuromyelitis Optica" is used (Wingerchuk et al., 2006a). These criteria state two absolute requirements and the requirement of two of three supportive criteria. The patient must suffer from optic neuritis and acute myelitis, as well as at least show either 1) a spinal cord lesion extending continuously at least over 3 or more vertebral segments 2) not MS-like brain MRI or 3) seropositive NMO-IgG status.

3.2. Histology

Characteristic lesions of NMO are mainly located in the spinal cord and show diffuse swelling and softening and extend over several vertebral segments. Active lesions show inflammation and infiltration of T-cells, B-cells and macrophages around vessels (perivascular cuffs) and throughout the lesion parenchymaa. Inflammation in these lesions is often associated with myelin loss, axonal damage, edema, as well as necrosis in grey and white matter. Additonally, infiltration of neutrophilic granulocytes and eosinophils can be observed (Lucchinetti et al., 2002; Misu et al., 2013). At the end feet of astrocytes perivascular deposition of immunoglobulin (Ig) and complement activation have been described. Additionally, AQP4 loss has been observed at these sites (Asgari et al., 2011).

Characteristic features of chronic lesions are gliosis and atrophy (Jarius et al., 2008).

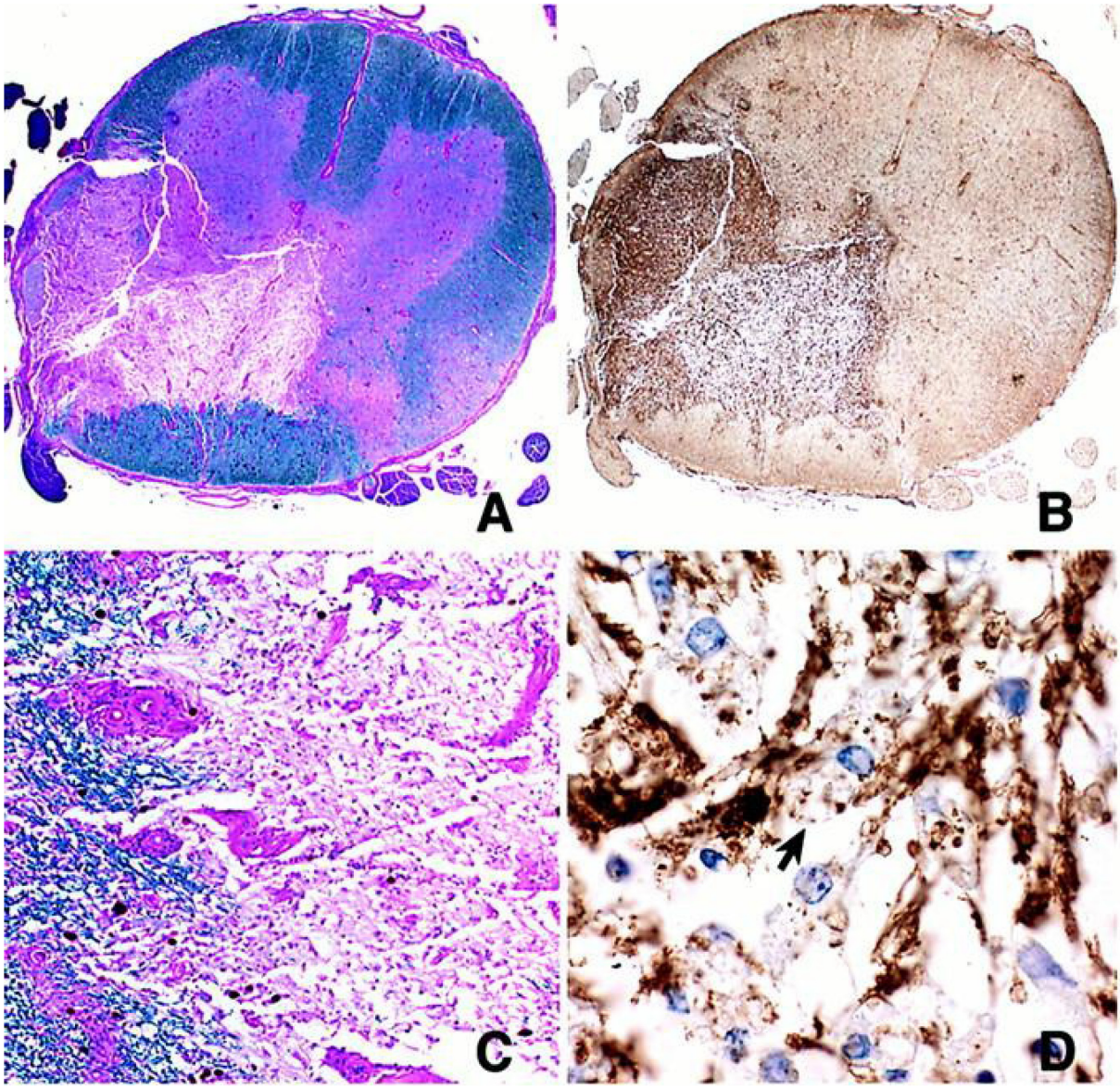

Figure 2: Histopathology of NMO. (A) Staining of the spinal cord cross-section with Luxol fast blue and PAS myelin stain demonstrates major demyelination affecting both grey and white matter (10x magnification). (B) The lesion is formed by numerous macrophages, which have been stained using KiM1P pan-macrophage stain (10x magnification). (C) One can distinguish very nicely between the periplaque white matter and the plaque after Luxol fast blue and PAS myelin stain (100x magnification). (D) As pointed out by the arrow macrophages contain myelin debris within their cytoplasm (MOG-Immunocytochemistry, 600x magnification). Figure was taken from (Lucchinetti et al., 2002) Copyright 2002, with permission from Brain.

3.3. NMO and MS

Multiple Sclerosis (MS) is a very heterogeneous demyelinating disease of the CNS caused by immune-mediated inflammation. This leads to axon damage and has patients suffer from loss of motor and sensory function (Karussis, 2014; Rice et al., 2013). There are not only various patterns of clinical course, to name a few relapsing-remitting, relapsing-progressive, primary progressive and secondary progressive, but also different immunopathological profiles.

Despite their similarities like optic neuritis and myelitis, which can be symptoms of both diseases, NMO and MS have mainly different characteristics. Thus it is of high importance to describe their differences in disease pathology, not least because drug therapy for MS cannot be directly applied to NMO and might exacerbate the disease (Fujihara et al., 2012). The prognosis for NMO is poor, the attacks are more severe, remission is incomplete and deficits accumulate. Important differences between NMO and MS are shortly summarized in Table 1.

A hallmark of MS is intrathecal synthesis of oligoclonal IgG bands, yet there is no associated biomarker to MS as there is for NMO since no target antigen has been found.

Characteristics	**MS**	**NMO**
Age of onset	29	39
Gender (F:M)	2:1	9:1 (no sex bias in monophasic course)
Clinical Features	85% remitting-relapsing 15% primary-progressive no monophasic course	80-90% relapsing course 10-20% monophasic course
Epidimology		
MRI	**brain**: periventricular white-matter lesions **spinal cord**: short-segmented peripheral lesions	**brain**: normal or non-specific white-matter lesions; 10% unique lesions (hypothalamic, corpus callosal, periventricular, brainstem lesions)

		spinal cord: longitudinally extensive central lesions (≥3 vertebral segments)
CSF white-blood-cells	mild pleocytosis, mononuclear cells	occasional prominent pleocytosis, polymorphonuclear cells and mononuclear cells
NMO-IgG	absent	68-91%
Oligoclonal bands	85%	15-30%

Table 1: Clinical differences between NMO and MS (Jarius et al., 2008; Nandhagopal et al., 2010; Wingerchuk et al., 2007)

3.4. Aquaporin-4

AQP4 belongs to the family of aquaporins which are selective water transporters, some aquaporins, called aquaglycerolporins, transport glycerol in addition. As the function suggests, AQP4 is a membrane protein with an aqueous pore, which consists of 6 transmembrane helices and 2 short non-membrane spanning helical segments surrounding the narrow aqueous pore. Both, the N-terminal and the C-terminal end reach into the cytosol. This gives rise to 5 loops, with loop A, C and E being extracellular and loop B and D intracellular (Yukutake and Yasui, 2010). Four monomers of about 30 kDa assemble to one tetramer (Pisani et al., 2011; Ratelade and Verkman, 2012). Multiple tetramers in turn, can assemble to large aggregates we call orthogonal array of particles (OAPs) (Landis and Reese, 1974; Rash et al., 1998; Verbavatz et al., 1997).

AQP4 is expressed in two major isoforms depending on which translation initiation site is used. One longer isoform (M1) with a translational start at the first methionine and one shorter isoform (M23) starting at the methionine at position 23 (Badaut et al., 2013; Graber et al., 2008; Levy et al., 2014; Ratelade and Verkman, 2012). While some antibodies bind to both isoforms with the same affinity, experiments have shown that AQP4-IgG generally binds to the M23 isoform with a higher affinity. (Ratelade and Verkman, 2012). Considering the small size of the water channel in comparison to the size of an IgG antibody (Figure 3B) the preference of the antibody for M23 suggests an actual binding to OAPs rather than to one single tetramer. OAP are formed by intermolecular interaction of residues downstream

of M23 and are stabilized by M23 while M1 does not form OAPs. And indeed, M23 isoform mutant human astrocyte cells do not form OAPs and show decreases antibody binding affinity (Crane et al., 2011).

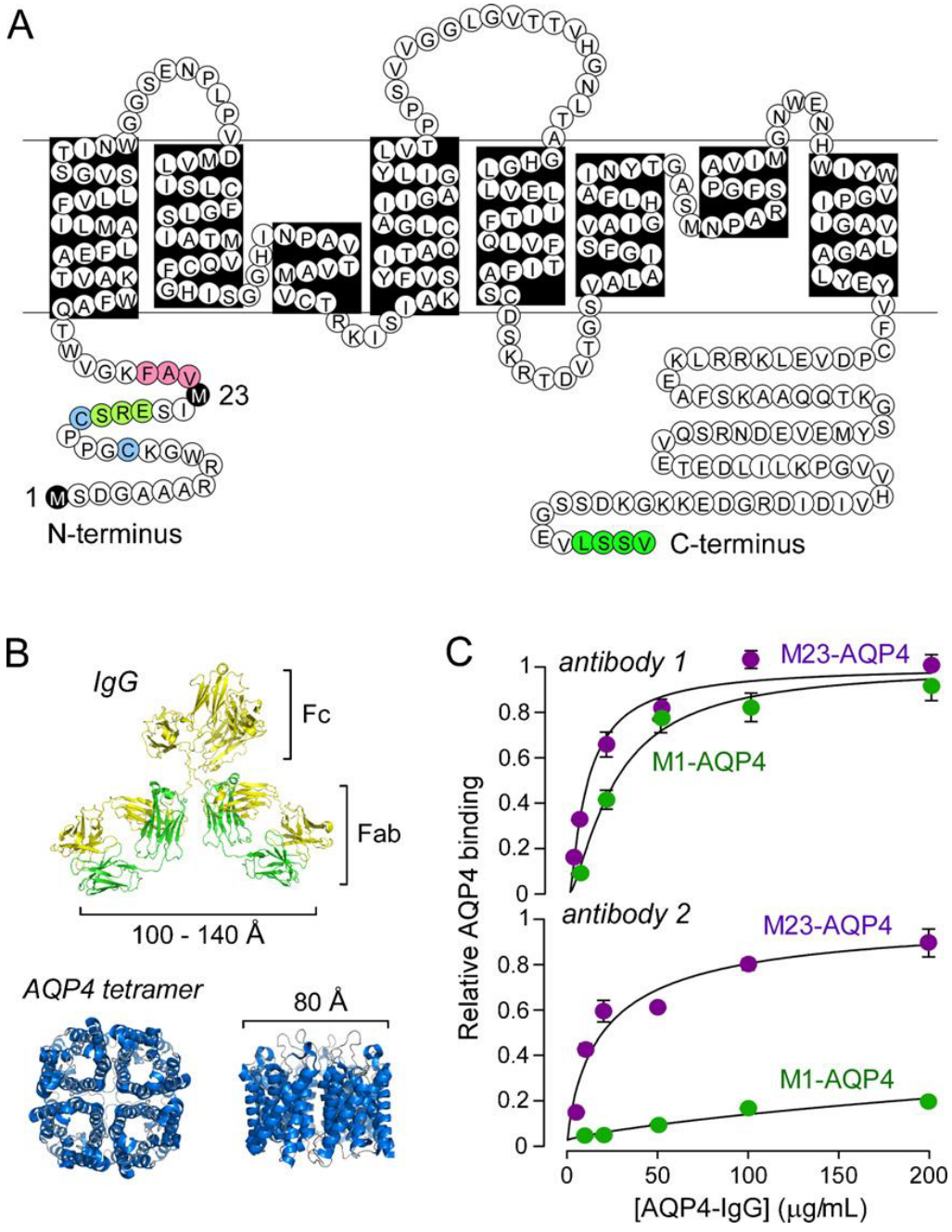

Figure 3: AQP4-IgG binding to its target, AQP4. (A) Amino acid sequence of human AQP4 showing Met-1 and Met-23 translation inhibition sites (black). Pink – residues involved in intermolecular N-terminus associations to form OAPs; light green – residues preventing OAP formation by M1-AQP4; blue – cysteine residues involved in palmitoylation- regulated OAP assembly; and dark green – C-terminus PDZ domain. (B) Crystal structure of human AQP4 (PDB, 3GD8) showing tetrameric association with central aqueous pore, along with structure of a generic IgG antibody shown on the same size scale. (C) Binding of two different monoclonal recombinant NMO autoantibodies to cells expressing M1-AQP4 or M23-AQP4. This figure was take from (Ratelade and Verkman, 2012). Copyright 2012, with permission from Elsevier.

M1 and M23 differ in translation initiation sites, but more isoforms have been identified formed by alternative splicing during AQP4 mRNA synthesis (Moe et al., 2008). In this work 4 additional isoforms have been found by rapid amplification of cDNA ends (RACE), but when expressing the isoforms in Xenopus oocytes to analyze the protein localization, it appeared as only one of the new isoforms (Mz), the longest, was transported to the cell membrane and is able to transport water. However, this isoform does not form OAPs and while it has been shown to interact with M23, it is unable to bind NMO-IgG and is not expressed in humans (Rossi et al., 2011).

Finding new isoforms of AQP4 is intriguing. We can only hypothesize about the function of the intracellular isoforms which do not make it to the cell membrane. Recently, the discovery of a new rat isoform and the first additional human isoform was reported (De Bellis et al., 2014). This isoform is a splice variant missing exon 4 and is not transported to the plasma membrane but has a negative-dominant effect on the full-length form. It is possible that this might be a method to regulate water transport in AQP4 expressing tissues.

3.5. NMO Pathology

After the discovery of NMO-IgG and its binding partner AQP4, a lot of research was published discussing the possible pathomechanism and the pathogenicity of the antibody and by which mechanisms the presence of these autoantibodies induce NMO disease pattern. Still, NMO pathology remains a highly complicated matter. A lot of conflicting data has been published and there is ongoing debate about the proposed disease mechanisms.

Characteristic features of lesions are AQP4 loss, perivascular and subpial deposition of humoral factors like IgG and IgM or activated complement (Misu et al., 2013). Additionally, recruitment of neutrophils and eosinophils can be observed. Judging from different lesion types, a wide spectrum of pathology must be involved.

Considering the existence of a disease-associated antibody and the parallel loss of GFAP, the involvement of astrocyte damage and humoral immunity is apparent, myelin damage on the other hand seems to be a secondary phenomenon as myelin and axonal neuronal axons are often preserved (Jarius et al., 2008; Levy et al., 2014). Interestingly, it appears some lesions develop in absence of complement activation and granulocyte infiltration (Misu et al., 2013). Thus, the pathology can be superficially divided in complement-dependent-cytotoxicity

(CDC) in presence of complement and antibody-dependent cellular cytotoxicity (ADCC) in absence of complement (Ratelade and Verkman, 2012). These mechanisms are both initiated by binding to the FC-region of the antibodies which can interact with the complement protein C1q (in CDC) and effector cell receptor FcR of Natural Killer (NK) cells (in ADCC).

When complement is activated granulocytes and activated macrophages are recruited, cytokines are released and the disruption of the Blood-Brain-Barrier (BBB) is promoted (Levy et al., 2014; Lucchinetti et al., 2002; Vincent et al., 2008). Astrocyte injury and inflammatory reactions such as neutrophil degranulations are believed to cause oligodendrocyte death, myelin loss and neuronal injury as a nonselective bystander destruction (Mitsdoerffer et al., 2013; Ratelade and Verkman, 2012). Injecting IgG from sera of NMO patients together with human complement in mice brain has been shown to produce NMO-like lesions including AQP4 and GFAP loss, vascolucentric deposition of activated complement components and

inflammatory cell infiltration as well as demyelination (Saadoun et al., 2010).

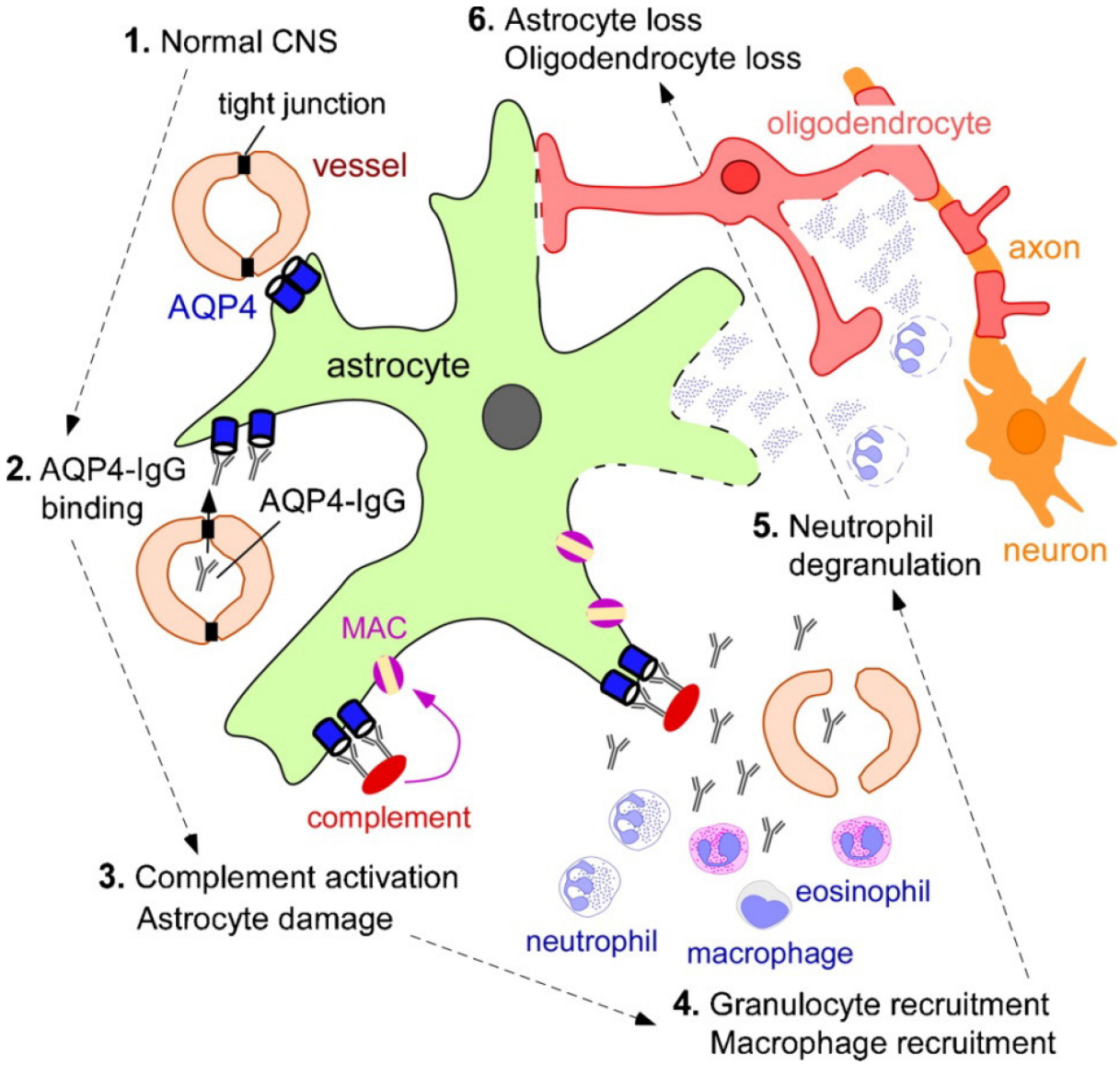

Figure 4: NMO pathogenesis mechanism. In the normal CNS, AQP4 is expressed at astrocyte end-feet facing the blood–brain barrier formed by endothelial cells connected by tight junctions (labeled '1'). In NMO, by an unknown mechanism, circulating AQP4-IgG crosses the blood–brain barrier and binds AQP4 on astrocytes (2). This leads to recruitment and activation of complement and deposition of the membrane attack complex (MAC), producing astrocyte damage (3). Complement activation and cytokine secretion by astrocytes recruit inflammatory cells (eosinophils, neutrophils and macrophages), which further disrupt the blood–brain barrier, allowing more entry of AQP4-IgG (4). Degranulating inflammatory cells (5) and astrocyte damage secondarily cause oligodendrocyte injury, myelin loss and axon damage (6). Figure and legend taken from (Ratelade and Verkman, 2012). Copyright 2012, with permission from Elsevier.

When NK cells are activated they release cytotoxic granules which contain perforin and granzymes causing apoptosis in target cells. NK cells in a complement-independent manner have shown to produce astocyte injury in mice (Ratelade et al., 2012), still histological evidence does not support involvement of NK cells and cytotoxic T-cells in NMO pathology based on the absence of granzyme B and perforin in human lesions (Saadoun, Samira, Bridges Leslie, Verkman A.S., 2013). When inhibiting complement activity in rats,

intracerebral injection of NMO-IgG does not cause the same severeness of lesions, but AQP4 loss can be observed around the needle track (Asavapanumas et al., 2013). ADCC may be involved in unique NMO pathology since evidence for complement-independent lesion formation in NMO has been reported (Misu et al., 2013).

There is conflicting evidence for endocytosis of AQP4 as another potential consequence of the binding of NMO-IgG to AQP4 and thus causing AQP4 loss in astrocytes (Hinson SR1, Pittock SJ, Lucchinetti CF, Roemer SF, Fryer JP, Kryzer TJ, 2007). These results, however, could not be replicated in mouse astrocyte cultures or living mice (Ratelade et al., 2011a) or rat astrocyte cultures (Asavapanumas et al., 2013).

3.6. Animal Models and T-cell involvement

Establishing a suitable animal model for NMO is of high importance for elucidating further disease mechanisms and developing new treatment therapies. As of today, there is no animal model for NMO which recapitulates human pathology and pathogenesis.

Peripheral injection of NMO-IgG has not proven to be successful to cause lesions in the brain or spinal cord unless the BBB was disrupted mechanically (Ratelade et al., 2011b). Intracerebral injection of NMO-IgG causes NMO-like lesions in mice but it is essential to coinject human complement (Saadoun et al., 2010) and therefore in consideration of the crucial role of complement activation in NMO, mice do not appear to be suitable model organisms.

In rats, the endogenous complement system can be used. And as already shown in mice, intracerebral injection of NMO-IgG causes NMO-like lesions, but can be performed without coinjection of human complement in rats (Asavapanumas et al., 2013).

NMO-IgG has been shown to worsen pathology when injected into rats with pre-existing inflammation caused by either immunization with CNS antigens (i.e. myelin basic protein) in complete Freund's adjuvant (Kinoshita et al., 2010) or transfer of activated CNS antigen specific T-cells (Bradl et al., 2009; Kinoshita et al., 2009).

One important factor seems to be the disruption of the BBB. Injecting NMO-IgG directly into the brain of model organisms does not explain how the antibody moves from the periphery to the brain. Not only is there a need for the antibody to pass the BBB, but also for

complement and activated effector cells. Bradl et al. elucidated the pathogenic potential of NMO-IgG in dependency of the disruption of the BBB. They show AQP4 and GFAP loss, inflammatory infiltrates, as well as Ig and complement deposition when injecting NMO-IgG into the periphery of EAE induced rats (Bradl et al., 2009). During the course of a MBP-T-cell mediated EAE the BBB is disrupted and allows the antibody and possibly other pathogenic components of the immune system to pass into the CNS. Injecting NMO patient-derived immunoglobulins which had been depleted of AQP4 antibodies into EAE induced rats leads to reduced pathology. They also show that administering NMO-IgG with nonencephalolitogenic T-cells do not lead to disease in rats. And interestingly, administering NMO-IgG in naïve, young rats with a leaky BBB does also not lead to disease in the animals (Bradl et al., 2009).

Judging from this data, we can hypothesize, that in addition to antibodies against AQP4, T-cells play a role in NMO pathogenesis. Besides complement deposition, IgG deposition has been observed in lesions (Brück et al., 2012; Lucchinetti et al., 2002). Therefore, it is evident, that AQP4 specific T-cells are part of the immune repertoire of NMO patients since B-cells need positive signals from helper T-cells for isotype switching from IgM to IgG (Litinskiy et al., 2002; Stavnezer). In fact, a study in Japanese NMO patients observed the clonal expansion of Vβ1 and Vβ13 chains of T-cell receptors (Warabi et al., 2006), another study observed an increased frequency of HLA-DPB1*0501, the human leukocyte antigen class II (HLA), in seropositive NMO patients (Matsushita et al., 2009). Those T-cells in the blood of NMO patients prove to have a bias towards Th17 polarization (Varrin-Doyer et al., 2012). Also recent data from our lab reports significantly more activated T-cells in early active NMO lesions compared to inactive lesions (Pohl et al., 2013). The number of activated T-cells in early active NMO lesion is also higher than in early active MS lesion. No significant difference in activated T-cells could be observed comparing early active to inactive MS lesions (Pohl et al., 2013).

To approach the role of AQP4-specific helper T-cells in NMO pathogenesis our lab has predicted potential T-cell epitopes on AQP4 based on the RT1.BL-peptide-binding motif since autoimmune-associated T-cell responses in Lewis rats are MHC class II RT1BL dependent (Wauben et al., 1997). We showed that AQP4-specific T-cells have encephalitogenic potential (Pohl et al., 2011). Neither when rats have been immunized with AQP4-peptides to

obtain antigen-specific T-cells, nor during the course of the AQP4-peptide specific T-cell induced EAE were clinical symptoms observed. Still, the T-cells cause a leaky BBB, migrate into the brain and spinal cord and cause inflammatory lesions along the entire neuraxis. The cells were able to recruit activated macrophages but no significant migration into the parenchymaa or astrocytic damage could be detected in absence of NMO-IgG coinjection. The cells rather formed densely packed foci on top of the intact subpial glia limitans. In combination with NMO-IgG injection AQP4 loss and more pronounced infiltration into the parenchymaa was seen. No inflammation in the optic nerve was detected and oligodendrocytes and myelin were not affected.

3.7. Neutrophils

As already mentioned, neutrophils and eosinophils infiltrate into lesions in NMO (Lucchinetti et al., 2002; Misu et al., 2007a; Wingerchuk, 2007). Neutrophils are part of the innate immune system and phagocytose bacteria and fungi (Segal, 2007). They are recruited by IL-17 (Miyamoto et al., 2003) and release granule protein and cytokines, proteases and reactive oxygen or nitrogen species and can therefore be one of the causes of bystander destruction leading to demyelination (Mitsdoerffer et al., 2013). Depleting neutrophils in mouse from the periphery has been shown to delay and sometimes even prevent EAE (McColl and Staykova, MA, Staykova MA, Wozniak A, Fordham S, Bruce J, 1998).

There is evidence for the further involvement of neutrophils in disease development. Neutropenia, that is reduced number of neutrophils in the blood stream, inhibits neuroinflammation when injecting NMO-IgG and human complement into mice brain (Vincent et al., 2013). Increasing the number of neutrophils by administering granulocyte-colony stimulating factor (G-CSF), that is inducing neutrophilia, exacerbated the lesions in the brain. This was confirmed by a recent report of a patient who experienced exacerbation of his first NMO episode after he was inadvertently given an injection with G-CSF (Jacob et al., 2012). Since G-CSF does not have an effect on MS patients, it appears that neutrophils play a key role in NMO pathology which has yet to be revealed.

3.8. Aim of work

So far, 2 different peptides were tested, $AQP4_{207–232}$ and $AQP4_{296-304}$ were tested and published(Pohl et al., 2011). We also tested $AQP4_{27-69}$ and $AQP4_{236–277}$ (data not published). To date, $AQP4_{207–232}$ which is part of the extracellular loop E with the predicted epitope

$AQP4_{220–228}$ (PAVIMGNWE) appears to be the peptide with the most encephalitogenic potential. What is the reason for this finding? Could this be explained by the absence of AQP4 isoform harboring loop E in the thymus? As previously mentioned, one AQP4 isoform generated by alternative splicing and missing exon 4, which codes for loop E, was detected in human muscle tissue (De Bellis et al., 2014). In the thymus T-cells undergo positive and negative selection to ensure self/non-self discrimination (Adam D. Griesemer1, Eric C. Sorenson1, 2011). One study observed the abundant presence of an isoform of Proteolipid Protein (PLP), which lacks 34 residues, in the thymus to cause a high susceptibility in SJL mice for PLP-specific EAE (Anderson et al., 2000). As it appears, by recognizing this particular region of PLP, the T-cells escaped tolerance and could become highly pathogenic.

Despite the dominance of loop E-specific T-cells, they fail to infiltrate into the parenchyma. There are three possible reasons for the lack of activation and infiltration of loop E specific T-cells. The antigen processing of AQP4 in the brain could result in a different peptide than those we have used to isolated helper T-cells. Another reason could be inefficient activation of $AQP4_{220-228}$ specific T-cells by macrophages and Dendritic cells due to low availability of AQP4 peptides at the blood-brain-barrier. And yet another possibility could be the low number of neutrophils since Lewis rats have a lower neutrophil count than humans (Johnson et al., 1999). The current work should address these questions.

4. Materials and Methods

4.1.Animals

Lewis Rats were used for all experiments. They were obtained from Charles River Wiga (Sulzfeld, Germany) and kept under standardized conditions in the Decentral Facilities of the Institute for Biomedical Research (Medical University Vienna). For immunization and passive EAE experiments female rats at an age of 8-10 weeks were used, for restimulation male and female rats of ages up to 6 months were used. The experiments were approved by the Ethics Commission of the Medical University Vienna and performed with the license of the Austrian Ministry for Science and Research.

4.2.Cells

T-cells together with antigen-presenting cells, like Dendritic cells and macrophages, were isolated from draining lymph nodes of immunized rats. They were kept in Restimulation Medium and were exposed to the antigen initially used during immunization. Antigen-specific T-cells recognize "their" antigen presented by Dendritic cells and macrophages and become activated. As a result of this, they express IL-2. These cells were then propagated in TCGF Medium which is high in IL-2 and thus favors proliferation and growth of antigen-activated CD4+ type 1 helper T-cells (Cantrell and Smith, 1983). With time IL-2 receptors of activated T-cells decrease. As a consequence, they do no longer respond to IL-2 and therefore stop proliferating. At this time point, the T-cells need restimulation, that is a new presentation of the antigen in the context of MHC class II products on the surface of antigen presenting cells. Antigen specific T-cells are then further expanded in number by alternating cycles of antigen specific T-cell activation and IL-2 dependent T-cell proliferation.

4.3.Antigen

Sequence of the peptide used for antigen-specific T-cell isolation and expansion of these cells: $AQP4_{207–232}$ (YTGASMNPARSFGPAVIMGNWENHWI) synthesized by Centic Bio- tech (Weimar, Germany).

Putative RT1.BL-binding epitope of this peptide: $AQP4_{220–228}$ (PAVIMGNWE)

4.4.Cell Culture

4.4.1. Solutions for Cell Culture

Antigen	2 mg/ml in RPMI
Complete Freund's Adjuvanz	4 mg/ml M. Tuberculosis H37Ra in incomplete Freund's adjuvans (Difco Laboratories, Detroit, USA), stored at 4C, shake well before use
ConA	Concanavalin A, 0.25mg/ml
Restimulation Medium	RPMI-1640 (Lonza) 1% L-Glu (200 mM in 85% NaCl solution, Invitrogen) 1% Penicillin/Streptomycin (10 000 U/ml + 10 000 U/ml Lonza) 1% Sodium pyruvat (100 mM Gibco) 1% Non-essential amino acids (100X Minimum Essential Medium, Gibco) 1% Rat-serum 0.2% β-Mercaptoethanol (99% Sigmal-Aldrich, diltued 1:1000 in RPMI)
TCGF Medium	RPMI-1640 (Lonza) 10% FCS (Lonza) 10% Supernatant of MLA cells producing murine IL-2 1% L-Glu (200 mM in 85% NaCl solution, Invitrogen) 1% Penicillin/Streptomycin (10 000 U/ml + 10 000 U/ml Lonza) 1% Sodium pyruvat (100 mM Gibco) 1% Non-essential amino acids (100X Minimum Essential Medium, Gibco) 0.2% β-Mercaptoethanol (99% Sigmal-Aldrich, diltued 1:1000 in RPMI)
Freezing Medium	RPMI-1640 (Lonza) 45% FCS (Lonza) 10% DMSO (Dimethyl Sulfoxide, Sigma)
4% PF	

4.4.2. Immunization

Female Lewis rats of 8-10 weeks were immunized with an emulsion containing 100 µl antigen [2mg/ml] and 100 µl Complete Freud's Adjuvans injected subcutaneously into the base of the tail of an anesthetized rat.

The rats were anesthetized in a chamber using 5% Isofluran and 4.5% O_2 and as soon as the rats were unconscious, the gas flow was decreased to 2% Isofluran.

4.4.3. Primary Cell Culture

On the 10^{th} day of immunization, the rats were sacrificed and the draining lymph nodes were extracted. Since we immunized the rats at the base of the tail, the antigen-specific T-cells can be found in the para-aortic lymph nodes. The animals were killed using CO_2 and the lymph nodes were extracted immediately. The abdomen was disinfected with 70% Ethanol and a V-shaped cut was made to access the lymph nodes. The lymph nodes were cut out of the fatty tissue that surrounds them and put into a 10 cm cell culture petri dish filled with sterile RPMI. The petri dish was stored on ice until the lymph nodes could be passed through a cell strainer (100 µm pores) into another 10 cm petri dish filled with 10-20 ml sterile RPMI to isolate the cells. The cell suspension was then taken up and pipetted into a 50 ml Tube. The dish was washed with another 10 ml of RPMI to minimize the number of cells left behind and the cell suspension in the Tube was centrifuged for 1 min for each ml RPMI used at 1300 rpm at 4 °C (Heraeus Megafuge 16R, Thermo Scientific). The supernatant was discarded and the pellet was resuspended in 5 ml Restimulation Medium and pipetted on a 60 mm cell culture petri dish making one dish for every sacrificed rat. Finally, 25 µl of antigen solution [2mg/ml] was added and the cells were incubated at 37 °C, 5% CO2 until they were activated. After 40-50 hours, the cells were fully activated. The cells increased in size and formed clusters of helper T cells surrounding antigen presenting cells (APCs). At this point, the cell suspension was centrifuged (1 min/ml, 1300 rpm, 4 °C) and the cell pellet was resuspended in TCGF Medium, a medium containing IL-2, and pipetted onto 10 cm dishes. After this, they could be again incubated at 37 °C, 5% CO2 for 4-6 days giving them time and space to proliferate while pipetting fresh TCGF onto the dishes or splitting them when needed.

4.4.4. Restimulation

After 4-6 days, the cells stopped proliferating and downregulate IL-2 receptors on the cell surface. Visually, they will decrease in size. To keep them alive and proliferating, they need to be restimulated. This is done by adding APCs and antigen and putting them on Restimulation Medium. The APCs are harbored from a thymus of another Lewis rat. For this, the gender of the rats is irrelevant.

The rats were killed using CO_2 and after the thoracic region of the rat was disinfected with 70% ethanol, the rat was cut open. Blood was withdrawn from the right hemisphere of the rat's heart using a 0,9x40mm needle and a 10 ml syringe for rat serum preparation. Then the thymus was removed using anatomical scissors and a small forceps. The thymus was immediately put on ice in a 10 cm petri dish filled with sterile RPMI.

Working in the cell culture hood, the thymus was pressed through a 100 µm cell strainer into a new 10 cm petri dish filled with fresh sterile RPMI. The cell suspension was then taken up and pipetted into a 50 ml tube and the dish was washed with 10 ml RPMI. The cell suspension was then put on ice and transported to the AKH Wien for irradiation (1 x 3000 rad) to damage the DNA of APCs and prevent them from proliferating. The APCs will continue to present the processed antigen to the T-cells for a few days and then die. After irradiation, the cells were centrifuged (1 min/ml) and the pellet was resuspended in 10 ml of Restimulation Medium for each thymus used.

The T-cells were pooled and centrifuged. The cells were either split 1:2 or 1:3 depending on the number of T-cells in the dish. The cell pellet was resuspended in 8 ml (1:2) or 12 ml (1:3) Restimulation Medium for each dish in the pool and each 4 ml of this cell suspension was pipetted onto a 60 mm dish. The restimulation was completed by adding 1 ml of APC cell suspension isolated from the thymus to each dish and 25 µl of antigen [2mg/ml]. This was incubated for 40-50 hours at 37 °C. When the cells looked fully activated they were centrifuged, resuspended in 10 ml TCGF Medium and put on 10 cm dishes. When the dishes were dense, they were split 1:2. After 4-5 days, the cells were in need for another restimulation.

4.4.5. Freezing Cells

The cells were centrifuged and the cell culture supernatant was discarded. The pellet was resuspended in 1-2 ml of Freezing Medium depending on the size of the pellet. This dense suspension was then pipetted into a 2 ml Cryo tube which was placed in a freezing box filled with Isopropanol and incubated at -80 °C for 48 hours. After this, the frozen cells were stored in liquid nitrogen.

4.4.6. Thawing Cells

The cells were thawed in a water bath at 37 °C. Then the suspension was diluted in 20 ml RPMI and centrifuged (1 min/ml, 1300 rmp, 4 °C), resuspended in TCGF and pipetted onto dishes depending on the number of dishes pooled, when they had been frozen.

4.5.Treatment with G-CSF

Filgrastim	recombinant human G-CSF, 30 Mio units/0.5 ml; Amgen, USA

Female rats at the age of 7-10 weeks were injected subcutaneously with 30 µg / kg G-CSF. The rats were not anesthetized for the injection, but it was rather done by pulling back the skin between the shoulders and injecting the solution under the skin. The first injection was done two days before the EAE was started and the injection was continued daily throughout the EAE experiment.

4.6.Passive EAE

For one animal 20 60 mm dishes which had been frozen as blasts were thawed and centrifuged (1 min/ml, 1300 rmp, 4 °C). The pellet was resuspended in 2 ml RPMI. The T-cells used had been restimulated 6 times and in the last of those restimulations ConA [0.25 mg/ml] was used instead of the antigen.

The rats were anesthetized using 5% Isofluran and 4.5% O_2 and then turned on their back pulling back their skin tightly to stretch the skin on their abdomen. Then the cell suspension could be injected carefully into their abdominal cavity. The rats were weighted and scored twice a day (Table 2).

Score	Clinical Symptoms
0	healthy

0.5	partial loss of tail tonus
1	complete loss of tail tonus
2	hind limb or fore limb paresis
3	hind limb or fore limb paralysis

Table 2: System used to describe the degree of symptoms seen in EAE

On day 7 the rats were sacrificed using CO_2 and perfused with 50 ml 4% PFA through the left ventricle. The animals were cut open and the brain, as well as spinal cord was dissected. In addition, samples from heart, lung, stomach, kidney, liver, spleen and muscle were taken. All the samples were incubated in 4% PFA for 18-24 hours at 4°C for further fixation. After this, they were stored in PBS at 4 °C until they were prepared for the staining.

4.7. Blood smear analysis to determine the number of neutrophilic granulocytes

After the rats had been sacrificed using CO_2, one drop of the rat's blood was extracted with a syringe and was smeared on a microscope slide. Then the preparation was allowed to dry. To reveal the nuclei of the peripheral blood mononuclear cells a May-Grünwald Staining was performed. First, the slides were incubated in May-Grünwald solution for 3 minutes. Then the smears were washed with ddH_2O and incubated in Giemsa solution (1:10) for 20 minutes. Finally, the slides were washed with ddH_2O.

4.8. Immunohistochemistry

4.8.1. Solutions for Immunohistochemistry

TBS (20x)	60.57 g TRIS (AppliChem) 180 g NaCl (Merck) 400 ml 1M HCl ad 1000 ml ddH_2O, pH 7.5
TBS (1x)	50 ml TBS (20x) 950 ml ddH_2O
PBS (4x)	13.8 g NaH_2PO_4 (Merck) 71.2 g g Na_2HPO_4 (Merck) 90 g NaCl (Merck)

	ad 2500 ml ddH_2O, pH 7.4
PBS (1x)	250 ml PBS (4x) 750 ml ddH_2O
H_2O_2/Methanol	150 ml Methanol 1 ml 30 % H_2O_2
EDTA Buffer (20x)	1.21g TRIS (AppliChem) 0.37 g EDTA (Merck) ad 50 ml ddH_2O, pH 9.1
EDTA Buffer (1x)	2.5 ml EDTA Buffer (20x) ad 50 ml ddH_2O
10% FCS in DAKO Buffer	10% FCS 90% DAKO Buffer (Dako Cytomation)
DAB (50x)	1 g 3,3'-Diaminobenzidine-tetrahydrochlorid Dihydrat (DAB) (Fluka) ad 40 ml PBS
DAB (1x)	1 ml DAB (50x) ad 50 ml PBS 16.5 µl 30% H_2O_2
Borate Buffer	0,154 g Boric acid (Merck) ad 50 ml ddH_2O, pH 8.0
CSA (1000x)	6 ml Borate Buffer 15 mg sulpho-NHS-Biotin (Pierce) 4.5 mg Tyramin (Sigma) stir over night, room temperature filter (0.45 µm)
CSA (1x)	20 µl CSA (1000x) 20 µl 30 % H_2O_2 ad 20 ml PBS

4.8.2. Tissue preparation and Immunohistochemistry

Brain and spinal cord were cut in serial section, both optic nerves were isolated as a whole and slices of the organs were put in chambers and dehydrated over night. Then the samples could be embedded in paraffin and cut in 2-4 µm thick sections on a microtome.

For staining, the sections were deparaffinized and rehydrated. This was done by incubating twice for 20 minutes with xylene and then in 96% ethanol. After this, they were incubated for 30 minutes in 0.1% H_2O_2 (in methanol), rehydrated by putting them in ethanol solutions with decreasing concentrations (first 96%, then 70%, then 50%) and finally, they were put in ddH_2O. For CD-3, ED-1 and AQP4 antibodies the sections needed pretreatment for epitope retrieval. This was done by steaming them in EDTA-Buffer for one hour. After washing with TBS, the unspecific binding sites were blocked by incubating the sections in 10% FCS in DAKO buffer for 20 minutes. Then the primary antibodies were applied for 1 hour at room temperature (Table 3) and after washing with TBS (3x) the biotinylated secondary antibody was applied for 1 hour at room temperature (Table 4).

Primary Antibody	Dilution	Stained Structure
CD-3 (rabbit, polyclonal, Neomarkers)	1:2000	T-cell receptor coreceptor
ED-1 (mouse, monoclonal, Serotec)	1:10 000	activated macrophages
AQP4 (rabbit, polyclonal, Sigma)	1:250	Intracellular AQP4 epitope
GFAP (mouse, monoclonal, Dako)	1:200	Glial Fibrillary Acidic Protein, Astrocytes

Table 3: Primary antibodies used for staining, diluted in 10% FCS in DAKO buffer

Biotinylated secondary Antibody	Dilution
sheep-anti-mouse (Jackson ImmunoResearch)	1:500
donkey-anti-rabbit (Jackson, ImmunoResearch	1:2000
donkey-anti-sheep/goat (Amersham/Healthcare)	1:200

Table 4: Dilutions of biotinylated secondary antibodies used for detecting primary antibodies, diluted in 10% FCS in DAKO buffer

To amplify the signal, the slides were incubated with CSA for 20 minutes on room temperature. This was washed with TBS (3x) and then treated with peroxidase-conjugated avidin (1:100 in 10% FCS in DAKO buffer) for 1 hour at room temperature. After washing

with TBS, the antibodies were detected using diaminobenzidine (DAB) and counterstained with Hematoxylin-Eosin (HE). After this, the slides were differentiated with 0.5% hydrochloride solution and incubated in Scott's solution for 5 minutes, then washed with water. Finally, the sections were dehydrated by incubating them in ethanol solutions with increasing concentration (first 50%, then 70% and 3 x 96%) and embedded in n-butylacetate.

4.9.Purification of RNA from tissue

4.9.1. Isolation of RNA

Lewis rats were killed using CO_2 and perfused with PBS after a piece thymus was taken out. The rat was skinned and the fasciae were removed slowly. Samples of at most 30 mg of selected tissues (thymus, soleus, flexor digitorum brevis, brain, and cerebellum) were extracted from Lewis rats, weighted and immediately put on dry ice.

The RNA was extracted using the QIAGEN RNeasy PLUS kit while working at room temperature using the Sigma 1-14 centrifuge (Linder Labortechnik). When using the kit for the first time some preparations have to be done. Before the isolation of RNA, β-mercaptoethanol was added to the RTL buffer (10 µl to 1 ml RTL buffer) and 96% ethanol was added to the RPE buffer.

The tissues were then homogenized in 600 µl RTL buffer using an electric tissue homogenizer and this lysate was pipetted on top of a QIAshredder spin column and spun at maximal speed for 2 minutes. The shredder was discarded and the flow through centrifuged for 3 minutes at maximal speed. The supernatant was pipetted on top of the gDNA Eliminator tube and spun for 30 seconds at 8 000 x g. The flow through was pipetted in volumes up to 700 µl into an RNeasy spin column and spun at 8 000 x g for 15 seconds. When exceeding 700 µl, the remaining volume can be pipetted into the same RNeasy spin column and the centrifugation step repeated. The flow-through was discarded after each centrifugation step. At this point all aliquots from one sample should be pooled by reusing the same RNeasy spin column. This column was washed with 700 µl RW1 buffer and spun at 8 000 x g for 15 seconds and the flow-through was discarded. Then 500 µl of RPE buffer was added and the column was spun at 8 000 x g for 15 seconds, the flow-through was discarded. After this, again 500 µl of RPE buffer were pipetted into the column but this time the column was spun for 2 minutes at 8 000 x g speed. To further dry the membrane, the column was placed into a

new collection tube and spun at maximal speed for 1 minute. To elude the RNA, the column was placed into a 1.5 ml tube and 50 µl of RNA-free water were pipetted into the column. This was centrifuged at 8 000 x g for 1 minute.

4.9.2. DNase Digestions

To remove potential genomic DNA contamination, DNase digestion was performed using Fermentas DNase. To 50 µl sample 20 µl of reaction mix was added (Table 5).

RNA sample	**50 µl**
DNase Buffer (10x)	7 µl
RiboLock RNase Inhibitor (Thermo Scientific)	2 µl
DNase 1	7 µl
RNase-free water	4 µl
Total volume	70 µl

Table 5: Reaction mix for one sample for DNase Digestion

This was mixed well, but not vortexed and incubated at 37 °C for 30 minutes. The reaction was the stopped by adding 7 µl Stop Solution EDTA and incubated at 65 °C for 10 minutes.

4.9.3. RNA Cleanup

To remove DNA fragments from this solution, the QIAGEN RNeasy kit was used again. 30 µl of RNase-free water were added to the samples and this volume was mixed with 350 µl RTL buffer. Then 250 µl of 96% ethanol were added and the sample was transferred into an RNeasy spin column and centrifuged at 8 000 x g for 15 seconds, washed with 500 µl RPE buffer, spun for 15 seconds at 8 000 x g and again washed with 500 µl RPE but centrifuged for 2 minutes at 8 000 x g. Then the column was dried by spinning at maximal speed for 1 minute and the RNA was eluted into a 1.5 ml tube with 30 µl RNase-free water by spinning for 1 minute at 8 000 x g.

The RNA samples were stored at -80 °C.

4.10. Reverse Transcription

The concentration of the RNA was determined by measuring the absorption at 260 nm using a spectrometer (Nanodrop 2000, Peqlab). Then the sample was diluted with RNase-free water to 1 µg/30µl. To this 2 µl of T7-N7 primers were added and the samples were incubated at 70 °C for 5 minutes and then on ice for 5 minutes (Table 6).

RNA sample	**30 µl**
+ T7-N7 primers	**2 µl**
M-MLV RT Buffer	10 µl
RiboLock RNase Inhibitor (Thermo Scientific)	2.5 µl
dNTPs	2.5 µl
RNase-free water	5 µl
Total volume	53 µl
+ M-MLV RT	2 µl

Table 6: Reaction mix for one sample for Reverse Transcription

After this 20 µl reaction mix was added to each sample followed by an incubation at 40 °C for 2 minutes. Next, 2 µl of M-MLV Reverse Transcriptase (Promega) was added and the samples were incubated at room temperature for 10 minutes. After this, the samples were incubated at 40 °C for 50 minutes followed by 15 minutes at 70 °C.

The DNA samples were stored at -20 °C.

4.11. PCR

Primer Pairs

AQP4 forward: ATTTTTGCCAGCTGTGAT

AQP4 reverse: CGTCTGCTGTGCAGCTTTGC

For the PCR the Peqlap Taq all inclusive kit and a Biometra Thermocycler (Tpersonal) were used. As suggested by the supplier, the primers were diluted in 384 µl (forward primer) and 463 µl (reverse primer) RNase-free water. 5 µl of DNA sample was mixed with 45 µl of reaction mix (Table 7) and then the amplification was started (Table 8).

DNA sample	**5 µl**

Buffer Y (10x)	5 µl
dNTP Mix	1 µl
Primer Forward	1 µl
Primer Reverse	1 µl
Taq Polymerase	0.5 µl
RNase-free water	35.5 µl
Total volume	50 µl

Table 7: Reaction mix for one sample for PCR

Program	Temperature	Duration
Initial Denaturation	95 °C	11 min
40 cycles of Denaturation	95 °C	30 s
Annealing	49 °C	30 s
Elongation	72 °C	30 s
Final Extension	72 °C	10 min

Table 8: PCR Program used to amplify AQP4 cDNA

4.12. Gelelectrophoresis

The PCR products were detected by Agarose-gelelectrophoresis. 10 µl of Loading Dye were added to the samples and mixed well by pipetting. Then the samples were loaded on a 2% Agarosegel (for preparation see Table 9) and the bands were separated at 100 V, 200 mA, 20 Watt for 45 minutes. As a size reference 10 µl of the invitrogen 100 bp DNA ladder were used.

2 % Agarose Gel	
Agarose	4 g
1 x TAE	200 ml
heat up in microwave (5 min)	
cool down with tap water	
Ethidium bromide (10 µg/ml)	8 µl

Table 9: Solution for 2 % Agarose Gel

5. Results

5.1. No evidence for the expression of mRNA of an AQP4 isoform missing exon 4

Recently, the expression of an additional AQP4 isoform generated by alternative splicing and missing exon 4 was shown in rat and human muscle tissue (De Bellis et al., 2014). We attempted to replicated these results and additionally analyze the expression of this particular AQP4 isoform in the thymus of the Lewis rat. For this, we extracted tissue samples from the soleus and Flexor digitorum brevis muscles (FDB), as well as samples from thymus of Lewis rats and isolated mRNA. After reverse transcriptions, we amplified exon 4 using primers in exon 3 and exon 5. The results are shown in Figure 5.

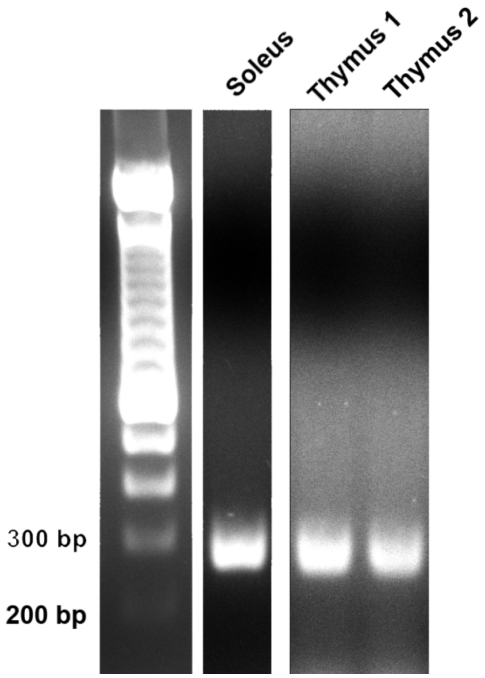

Figure 5: PCR amplification of a sequence of AQP4 containing exon 4. For the negative control water was used instead of template. The products of AQP4 isolated from thymus are samples from 2 different Lewis rats. We do not see a band at 218 bp.

We can only show the expression of one isoform in Lewis rat thymus and cannot confirm the expression of a second isoform in soleus (Figure 5) or FDB muscle (data not shown). The band we see is about 290 nucleotides long suggesting that this is isoform which includes exon 4, since this fragment has a size of 299 nucleotides whereas the isoform with the deletion of exon 4 has a size of 218 nucleotides.

5.2. Confirming the minor encephalitogenic potential of loop E-specific T-cells

Lewis Rats were immunized with loop E of the rat AQP4 protein. After 10 days, T-cells were isolated from the draining lymph nodes and expanded in number by alternating cycles of antigen-driven T-cell activation and IL-2 driven T-cell proliferation. This resulted in a pure population of antigen-specific type 1 helper T-cells. After 6 of these cycle ("restimulations"), the cells were injected into the abdomen of Lewis rats to induce an EAE. At the peak of the disease (i.e. on day 6 after T-cell transfer), the animals were sacrificed and brain, spinal cord as well as organs were extracted and stained.

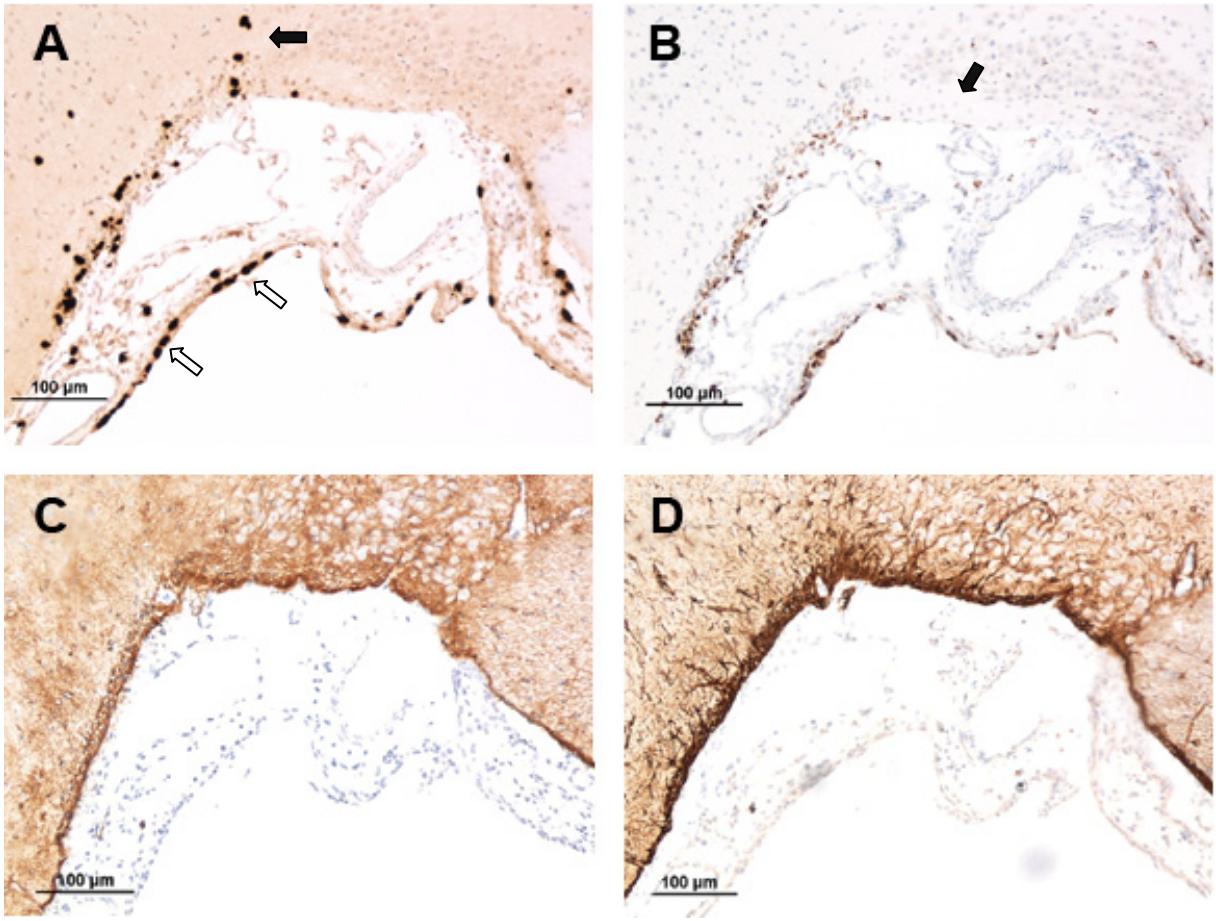

Figure 6: CNS lesion causes by $AQP4_{207-232}$-specific T-cells. The lesion is located close to the hippocampus**.** CD-3 staning of T-cells. Some are caught in the meninges (white arrows), others have begun to infiltrate into the parenchyma (black arrow) (A). ED-1 staning of macrophages. Macrophages colocalize with T-cells. Absence of macrophages in absence of T-cells (black arrow). Macrophages do not follow infiltrating T-cells (B). AQP4 staining of nervous tissue. No AQP4-loss observed (C). GFAP staining of astrocytes. We do not observe GFAP loss, therefore no astrocyte damage is caused (D).

The results of these experiments confirm our previous findings. Neither did the rats lose weight, nor show any clinical signs of EAE. Still, the injected T-cells migrated to the brain and the spinal cord and caused small inflammatory lesions along the entire neuraxis (Figure 6A, Supplementary Figure 1). These lesions contained only few macrophages (Figure 6B). We do

not observe AQP4 loss or GFAP loss (Figure 6C and D) at the lesion sites. We observed T-cells in the cerebral and cerebellar cortex. At these sites, the T-cells essentially remained in the meninges and did not penetrate into the parenchyma (Figure 7).

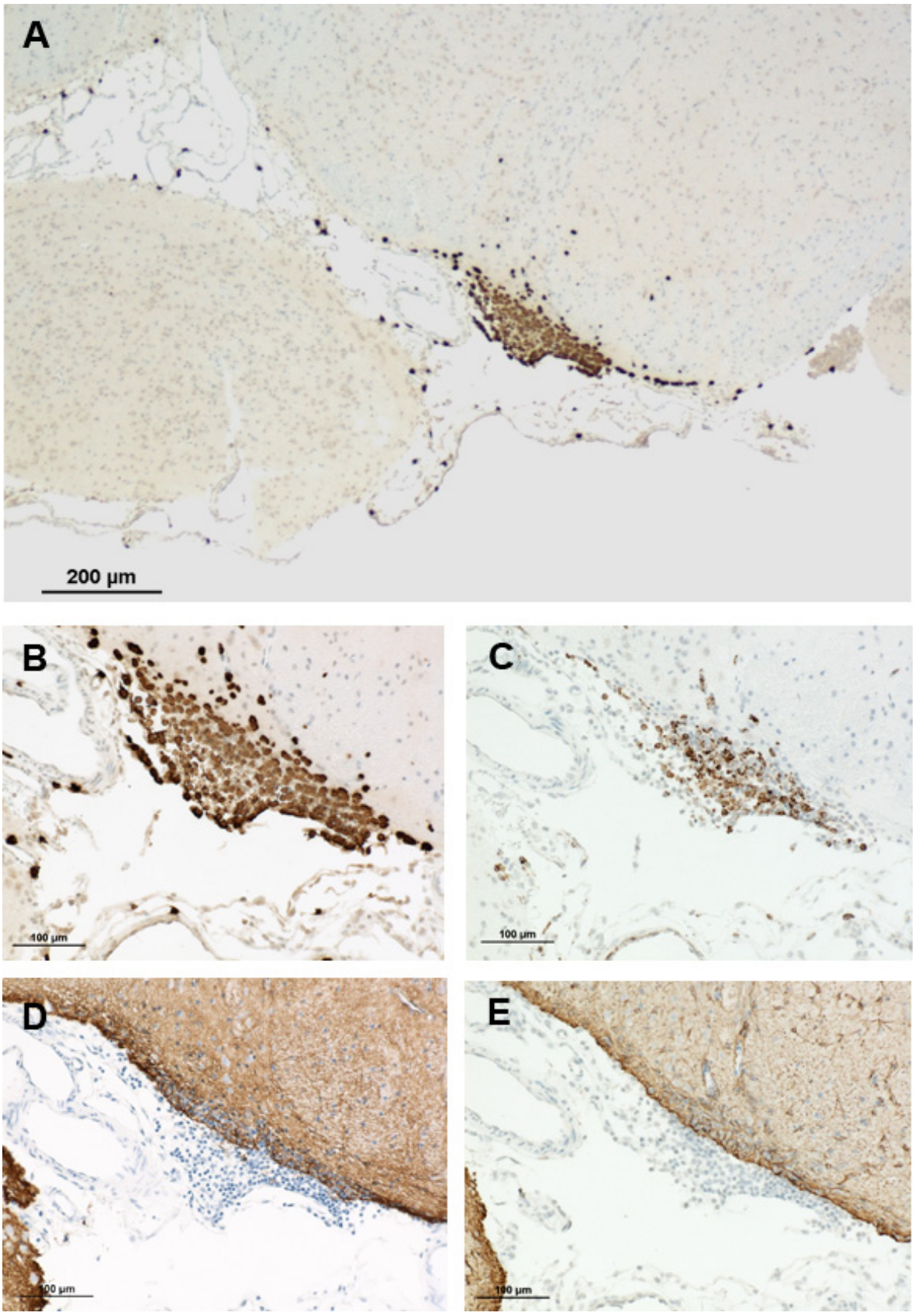

Figure 7: Inflammatory cells forming foci in lesions caused by AQP4$_{207-232}$-specific T-cells. The lesion is located close to the hippocampus**.** CD-3 staning of T-cells. Overview of the lesion (A). Higher magnification of the CD-3 staining. Very few cells migrate into the parenchyma, most cells sit on top of each other and seem to be inhibited from rupturing the glia limitans (B). ED-1 staining of macrophages. Macrophages colocalize with T-cells. Few mcrophages follow infiltrating T-cells (C). AQP4 staining of nervous tissue. No AQP4-loss observed (D). GFAP staining of astrocytes. We do not observe GFAP loss and there no evidence of astrocyte damage (E).

5.3. No increased T-cell infiltration when raising the neutrophil count

To address the involvement of neutrophils in AQP4-specific T-cell EAE, we used daily injections of G-CSF to increase the number of neutrophils in the blood stream of Lewis rats. By administering 30 µg/kg of G-CSF we almost doubled the number of neutrophils in relation to the number of white blood cells (WBCs) in animals without EAE (Figure 8, Supplementary Figure 2). During the course of an EAE G-CSF and other inflammatory mediators cause the number of neutrophils to increase. This can be seen in the control animals, which have only been treated with PBS. When treating EAE-animals with G-CSF the ratio of neutrophils only further increased in 2 animals. The other 2 animals show a neutrophil/WBCs ratio in the bloodstream comparable to PBS treated animals with no EAE induction.

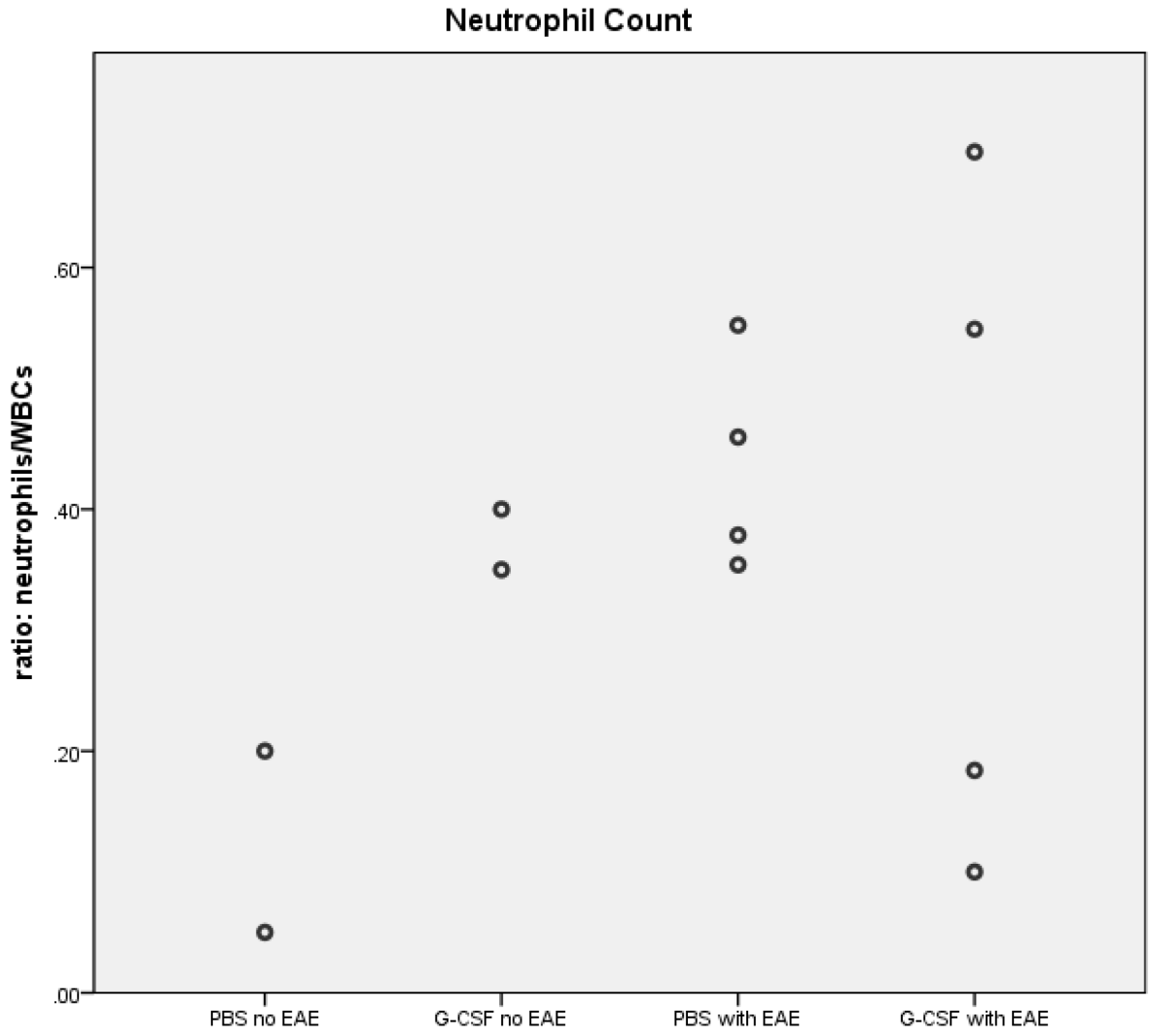

Figure 8: Graph showing the ratio of neutrophils to white blood cells (WBCs). PBS no EAE: Lewis were injected daily with PBS. G-CSF no EAE: Lewis rats were injected daily with G-CSF. PBS with EAE: Lewis rats were injected daily with PBS, on day

3 $AQP4_{207-232}$-specific T-cells were injected to start EAE. PBS with EAE: Lewis rats were injected daily with G-CSF, on day 3 $AQP4_{207-232}$-specific T-cells were injected to start EAE.

In theory, the relative low number of neutrophils in the bloodstream could indicate increased migration of these cells into the brain or spinal cord as a response to EAE. However, we do not see more neutrophils in lesions of animals with low neutrophil counts than in rats with G-CSF increased neutrophil number (Figure 9). Thus, we cannot infer that neutrophils had been recruited into the brain and are therefore low in number in the bloodstream. In these animals neither the EAE, nor G-CSF seem to be able to stimulate neutrophil differentiation. The reasons for this finding remain unclear.

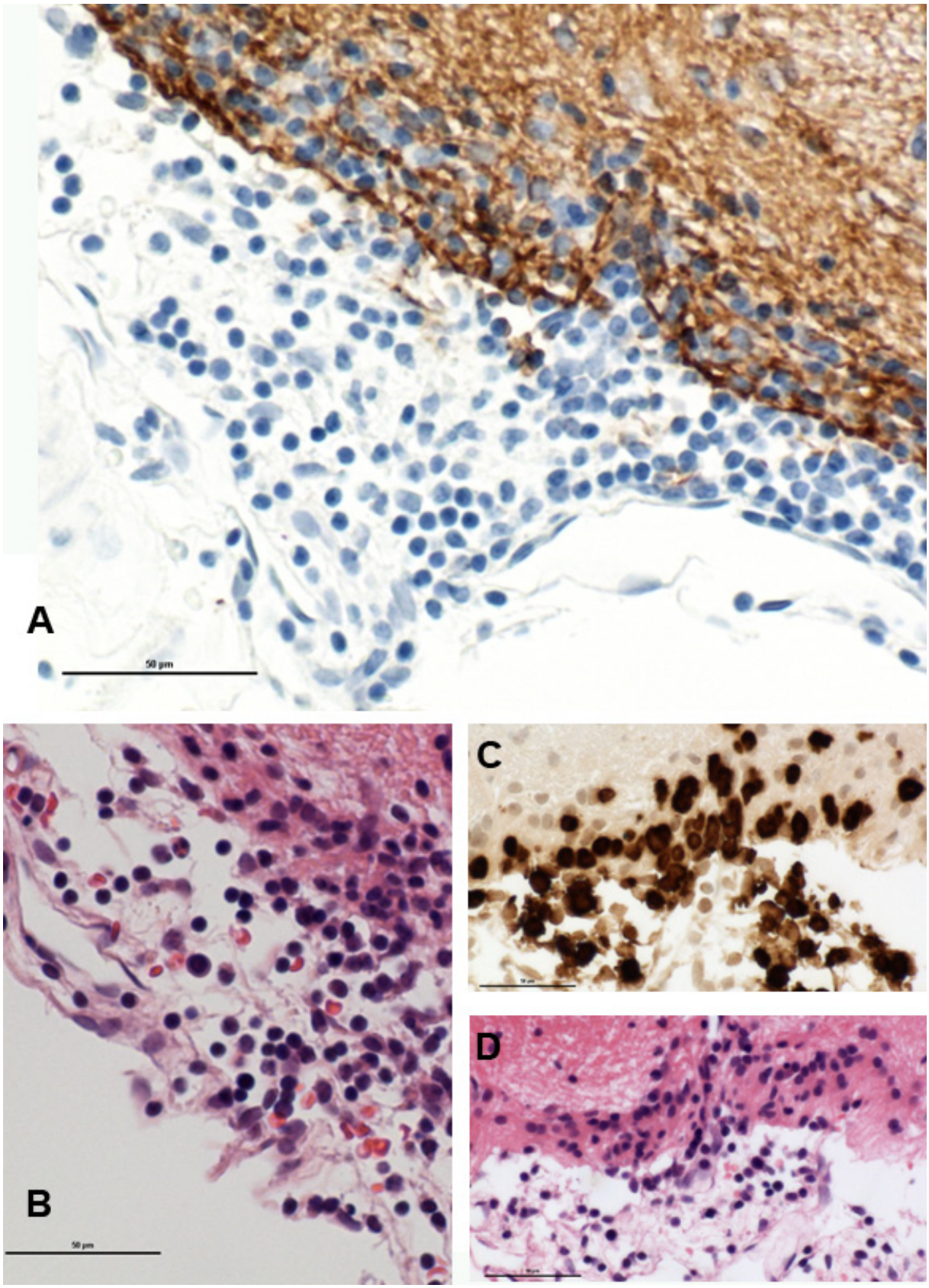

Figure 9: G-CSF treated rats with low neutrophil count in the blood stream do not show an elevated number of neutrophils in lesions in the brain. AQP-4/HE staining of piled up inflammatory cells in a G-CSF treated rat with low neutrophil number in the blood stream (A). HE staining of the lesion shown in A (B). CD-3 staining of a lesion in a G-CSF treated rat with elevated neutrophil number in the blood stream (C). HE staining of the lesion shown in C (D).

Regardless of the neutrophil/WBCs ratio, raising the neutrophil count in the bloodstream of Lewis rats does not change the localization of inflammatory lesions (Figure 10). More importantly, G-CSF treatment does not lead to significant T-cell infiltration into the parenchyma during passive EAE. T-cells are either piled up in dense foci (Figure 7) or remained trapped in the meninges (Figure 10C). There are only few lesions depicting infiltrating T-cells and these few lesions cannot be linked to either G-CSF or PBS treatment. Figure 10E shows T-cells beginning to infiltrate into the parenchyma in a rat treated with G-CSF and Figure 10F depicts the same effect in PBS treated control rats. T-cells tend to be trapped in the meninges independently of PBS/G-CSF treatment.

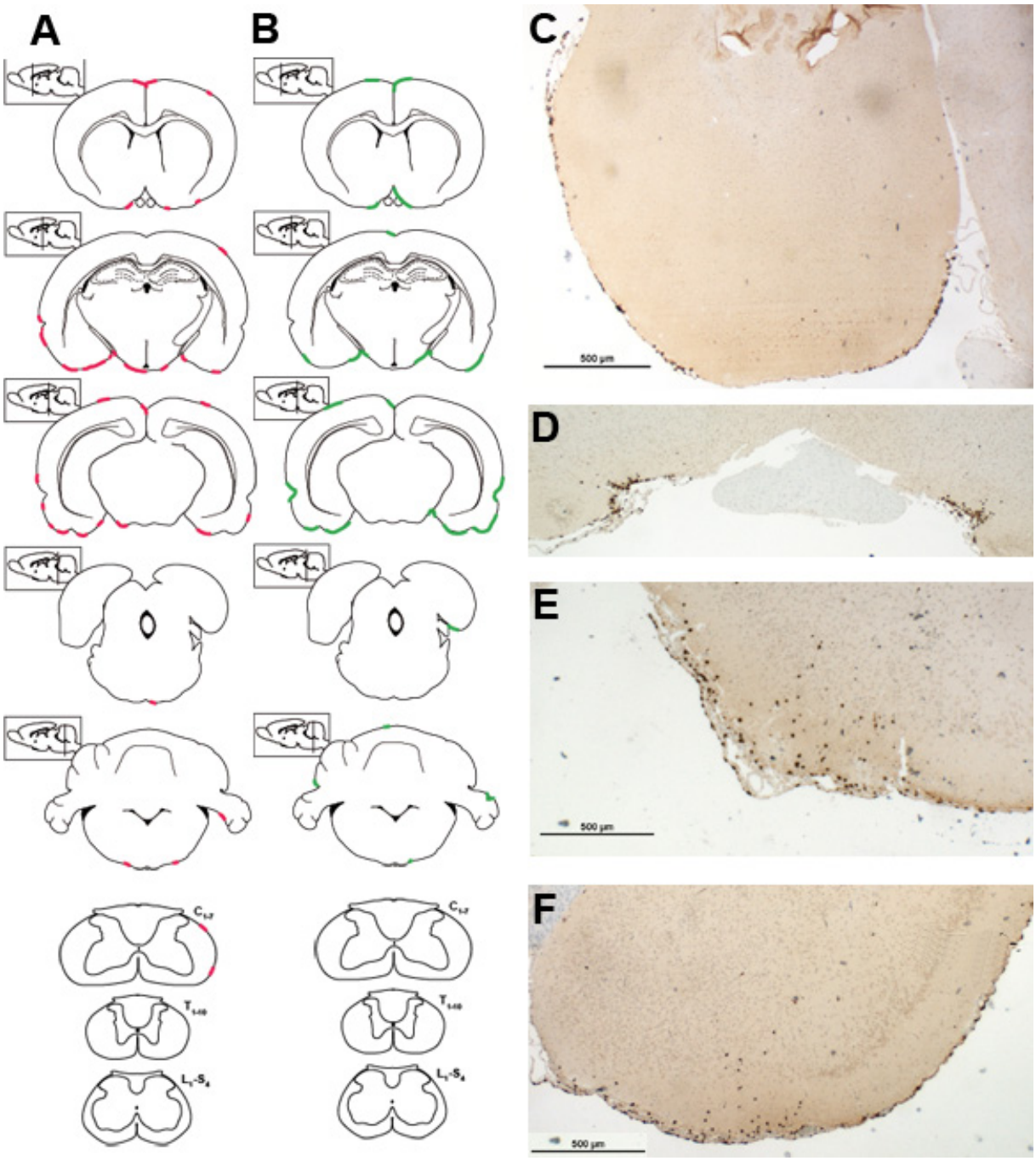

Figure 10: Localization of T-cellsin the CNS at the peak of an antigen-specific EAE. The localization of T-cells is shown using schemes provided by (Paxinos G, 1997). Localization of T-cells injected in G-CSF treated rats (A). Localization of T-cells injected in PBS treated control rats (B). CD-3 staining of rat brain (C-D). Trapped T-cells in the meninges of the cortex close to the hippocampus in G-CSF treated rats (C). T-cells slightly infiltrating the parenchyma close to the ventricles, internal capsule (ic) and the CA1 field of the hippocampus in G-CSF treated rats (D). T-cells beginning to infiltrate the parenchyma in the cortex close to the hippocampus in G-CSF treated rats (E). T-cells beginning to infiltrate the parenchyma in the cortex close to the hippocampus in PBS treated control rats (F).

6. Discussion

NMO pathology has yet to be fully understood. The discovery of the presence of NMO-IgG, a pathogenic antibody that targets AQP4 channels, has enabled the establishment of a disease model that combines results from animal experiments with histological findings. The antibodies interact with complement and activated inflammatory cells such as T-cells, macrophages, neutrophiles and eosinophils are recruited to the lesion sites (Lucchinetti et al., 2002). There are animal models in rat and mouse focusing on antibody and complement interaction and pathological consequences arising from this interaction but little is known about the disease pathogenesis (Asavapanumas et al., 2013; Saadoun et al., 2010). Neither complement nor inflammatory cells can pass an intact Blood-Brain-Barrier (BBB). Activated T-cells can pass the BBB and by providing proinflammatory mediators they enable inflammatory cells to infiltrate the tissue (Bartholomäus et al., 2009).

AQP4 peptide-specific T helper cells are assumed to be part of the immune repertoire of NMO patients since epitope-specific T-cells have to interact with B-cells in order to switch the isotype of antibodies to IgG (Litinskiy et al., 2002). Clonal expansion of Vβ chains of T-cell receptors has been described in seropositive Japanese NMO patients (Warabi et al., 2006). More importantly, not only have AQP4 peptide-specific T-cell been isolated from the periphery of NMO patients and healthy controls but AQP4-specific T-cells from NMO patients exhibit greater proliferation when presented AQP4 epitopes than those from healthy controls (Varrin-Doyer et al., 2012).

However, the pathogenicity of AQP4-specific T-cells in humans is unclear. We have tested the encephalitogenic potential of AQP4-specific CD4+ T-cells using 4 different peptides of AQP4 (Pohl et al. 2011, unpublished data) which have been predicted to be potential T-cell epitopes since they are suitable RT1.BL binding motifs (Wauben et al., 1997). While only causing subclinal EAE, AQP4 specific T-cell mediated EAE seems to result in most lesions, when $AQP4_{207-232}$-specific T-cells were used (Pohl et al., 2011). One potential reason for this dominance of one particular peptide could be the ability of T-cells specific for this peptide to escape negative selection in the thymus because of a dominantly expressed isoform of AQP4 in the thymus which lacks the region corresponding to the peptide which is specifically recognized by those T-cells. This phenomenon was described in PLP-mediated EAE in SJL mice (Anderson et al., 2000). The abundant expression of a shorter PLP isoform in those

mice allowed for a high susceptibility for PLP-specific EAE using a peptide which was not present in the thymus.

Recently, another isoform of AQP4 in human and rat was identified (AQP4Δ4) (De Bellis et al., 2014). Since this isoform lacks exon 4 and does not code for loop E we investigated whether this isoform could be present in the thymus of Lewis rats. We isolated RNA from different tissues including the Soleus and Flexor Digitorum Brevis (FDB) muscle and after reverse Transcription performed a semi-quantitative PCR of regions flanking exon 4. Soleus and FDB have been shown to express AQP4Δ4 in addition to the canonical M1 and M23 isoforms in human and male Wistar rats (De Bellis et al., 2014). We, however, report controversial results. We detected the expression of only one isoform in Soleus (Figure 5) and FDB muscle (data not shown). We also do not detect the expression of another isoform in any of the 6 thymus samples we obtained from 6 different Lewis rats. It is possible that AQP4Δ4 is absent in Lewis rats but present in Wistar rats (used in the de Bellis study (De Bellis et al., 2014)) and humans. Another discrepancy is the amount of templated RNA used for reverse transcription. De Bellis et al. used double the amount of RNA as we did for our experiments. Still, they can only detect AQP4Δ4 in very low amounts in the tissue (Figure 11).

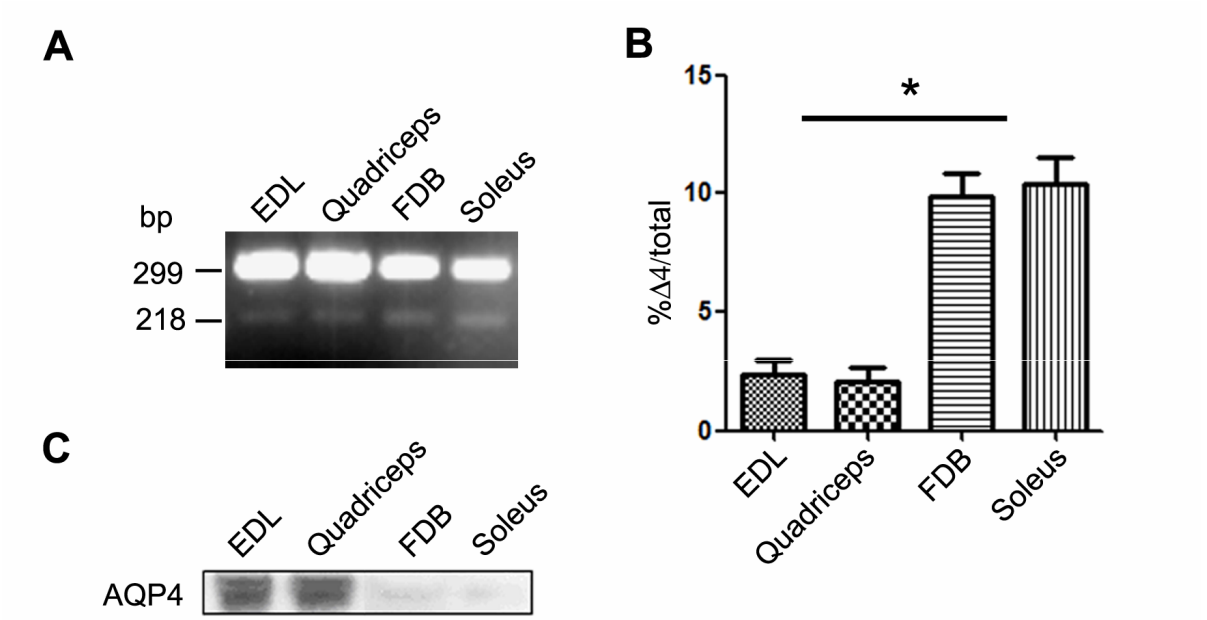

Figure 11: Expression of AQP4-Δ4 in rat skeletal muscles. (A) Co-amplification by RT-PCR of AQP4 splice variant with full length AQP4 from rat Exstensor digitorum longus (EDL), quadriceps, FDB and Soleus muscles and cerebellum. Note the two bands visible in skeletal muscles. Densitometric analysis of AQP4-Δ4 abundance in different muscles (*P<0.05, n=3) (B). (C) Immunoblot analysis of AQP4 expression in the analyzed rat tissues. Figure and legend taken from (De Bellis et al., 2014). Copyright 2014, Free via Creative Commons 2 months after publication.

So it is still possible that AQP4Δ4 is expressed in Lewis rat tissue but in low amounts. This quantity of expression of AQP4Δ4 is irrelevant for our experiments, since AQP4Δ4 but not AQP4 has to be expressed at a significant quantity in the thymus to play a role in T-cell tolerance. This means, the observed dominance of loop E-specific T-cells does not arise from the absence of loop E in the thymus.

After testing the pathogenic potential of multiple predicted epitopes of AQP4 for helper T-cells presentation loop E has shown to be the epitope with the highest pathogenic potential (Pohl et al. 2011; data not shown). Still, loop E specific T-cell mediated EAE only causes a subclincal disease. The T-cells reach the brain and spinal cord, but essentially remain within the meninges of the perivascular space and do not infiltrate the parenchyma (Pohl et al., 2011). We investigated the potential influence of neutrophils in loop E specific T-cell mediated EAE in Lewis rats. Neutrophils are part of the infiltrating cells in NMO lesions (Misu et al., 2007b), and a reduced number of neutrophils has been shown to inhibit inflammation in mouse brains whereas an increased number of neutrophils has been shown to cause more severe lesions in mouse brains (Vincent et al. 2013; McColl et al. 1998). Generally, neutrophils are involved in the recruitment, activation and programming of APCs (Nathan, 2006) and there is evidence for the ability of neutrophils to promote Th1 development (Bennouna et al., 2003). Neutrophils are generated in the bone marrow and can be recruited by granulocyte-colony stimulating factor (G-CSF). G-CSF is produced by monocytes, fibroblasts and endothelial cells and regulates the release of neutrophils from the bone marrow, neutrophil progenitor proliferation and differentiation and neutrophil activation (Anderlini et al., 1996; Demetri and Griffin, 1991).

We treated Lewis rats with G-CSF and aimed to double the number of neutrophils in the periphery of these rats. We achieved the elevation of the number of neutrophils in animals treated with G-CSF compared to control animals treated with PBS independent of EAE induction (Figure 8). The number of neutrophils in the blood stream of PBS treated rats with induced EAE is comparable to the number of neutrophils in G-CSF treated animals without the induction of EAE. This is not surprising, since the induction of EAE stimulates inflammation and thus induces the proliferation and differentiation of immune response cells. Curiously, in two animals, the number of neutrophils was neither raised by the EAE induced inflammation, nor by the administration of G-CSF although these animals showed

evidence for meningal inflammation. For unknown reasons, we could not increase the number of neutrophils in the periphery of these rats.

Independently of G-CSF or PBS administration and treatment effectiveness, we do not observe significant infiltration of the parenchyma in any of the animals. The T-cells remain in the meninges, sites of infiltration of T-cells are rare and found in the same quantity in all animals (Figure 10). The T-cells recruit macrophages (Figure 6B and Figure 7C), but T-cells and macrophages either pile up (Figure 7) or distribute over the whole neuroaxis (Figure 10C). However, neutrophils do not get recruited to those lesions (Figure 9).

We use helper T cells type 1 for the induction of EAE. There is evidence for the involvement of helper T-cells type 17 in NMO. T-cells in NMO patients have been found to be predominantly subtype 17 (Varrin-Doyer et al., 2012) and patient CSF shows elevated levels of IL-17 (Ishizu et al., 2005) and IL-8, which recruits neutrophils (Uzawa et al., 2010). It is possible that Th1 inherently recruit less neutrophils, than Th17 cells do. However, it has been shown that T-cells have to be activated to infiltrate the parenchyma (Pohl et al., 2013). To recruit effector cells, such as neutrophils, to the lesions T-cells have to be activated as well. So, the ability of the T-cells to recruit neutrophils is not relevant as long as they are not able to infiltrate the parenchyma. Therefore, we can infer with high certainty that the mere presence of higher numbers of neutrophils in the blood stream and the interactions which arise from that do not enable Th1 cells to infiltrate the parenchyma.

This raises one important question. Does the endogenous processing of the AQP4 in rats result in a different dominant epitope? If this is the case, loop E would not be present in sufficient amounts to enable the activation of loop E-specific T-cells in vivo. This would be in contrast to the situation in vitro where the loop E peptide is readily available for the activation of T-cells. Since the encephalitogenicity of T-cells creucially depends on their activation status in vivo (Kawakami et al., 2004). A low availability of loop E peptide in local APCs could limit T-cell re-activation at this site and hence prevent T-cell immigration into the parenchyma.

7. Conclusion and Outlook

Loop E-specific T-cells appear to cause more inflammatory lesions during AQP4-specific T-cell mediated EAE in Lewis rats than all other AQP4-specific T-cells tested so far. The dominance of loop E-specific T-cells when mediating EAE using AQP4-specific T-cells in Lewis rats cannot be explained by an intratyhmically expressed AQP4 isoform not including loop E.

Loop E-specific T-cells still fail to cause clinical symptoms during EAE. Based on my results, we could not increase this subclinical pathogenic potential of loop E-specific T-cells by raising the number of neutrophils in the blood stream of Lewis rats. This treatment did not enable loop E-specific T-cells to migrate into the parenchyma.

The reason for the low pathogenic potential may rather depend on the limited availability of this specific epitope in perivascular Dendritic Cells and macrophages of the CNS. If this is the case, application of the loop E peptide into the CSF of animals with ongoing AQP4-loop E-peptide specific T-cell EAE should result in T-cell migration into the CNS parenchyma.

8. Acknowledgements

I have to thank Assoc. Prof. Dr. Monika Bradl for giving me the opportunity to work in her group. Without her this thesis would not have been possible, but I have to thank her mostly for her patience and guidance. Next, I want to thank Prof. Dr. Hans Lassmann for allowing me to work in his lab.

I am very grateful for the help and patience of our technical assistance, Marianne Leißer, Ulrike Köck and Angela Kury. My special thanks go to Nikolaus Kögl who has helped supervising me, introduced me to the techniques. I want to thank him for his support, motivation and friendship. Next, I want to tank Maja who has guided me through big parts of my thesis, scientifically and personally. Of course, I have to thank for Maria's and specially Antonia's help, without who I would have been working in the lab until midnight on some (poorly planned) days. I have to thank Conny who was always there for my questions even if she was not in charge of me, Simon for his help and discussions, Joana for her friendship Lukas and Tobias for always cheering me up. I also want to thank Satoru and Taro.

I want to thank my family for supporting me through my studies. My mother for always giving me a push when I needed it (and not needed it), my father for believing in me and my two sisters and brother for taunting me like siblings do.

Finally, I have to thank my partner, Shahin, and my best friend, Steffi, for supporting me through life.

9. References

Adam D. Griesemer1, Eric C. Sorenson1, and M.A.H. (2011). The Role of the Thymus in Tolerance. *90*, 465–474.

Anderlini, P., Przepiorka, D., Champlin, R., and Körbling, M. (1996). Biologic and clinical effects of granulocyte colony-stimulating factor in normal individuals. Blood *88*, 2819–2825.

Anderson, a C., Nicholson, L.B., Legge, K.L., Turchin, V., Zaghouani, H., and Kuchroo, V.K. (2000). High frequency of autoreactive myelin proteolipid protein-specific T cells in the periphery of naive mice: mechanisms of selection of the self-reactive repertoire. J. Exp. Med. *191*, 761–770.

Argyriou, a a, and Makris, N. (2008). Neuromyelitis optica: a distinct demyelinating disease of the central nervous system. Acta Neurol. Scand. *118*, 209–217.

Asavapanumas, N., Ratelade, J., and Verkman, a S. (2013). Unique neuromyelitis optica pathology produced in naïve rats by intracerebral administration of NMO-IgG. Acta Neuropathol.

Asgari, N., Owens, T., Frøkiaer, J., Stenager, E., Lillevang, S.T., and Kyvik, K.O. (2011). Neuromyelitis optica (NMO)--an autoimmune disease of the central nervous system (CNS). Acta Neurol. Scand. *123*, 369–384.

Badaut, J., Fukuda, A.M., Jullienne, A., and Petry, K.G. (2013). Aquaporin and brain diseases. Biochim. Biophys. Acta - Gen. Subj.

Bartholomäus, I., Kawakami, N., Odoardi, F., Schläger, C., Miljkovic, D., Ellwart, J.W., Klinkert, W.E.F., Flügel-Koch, C., Issekutz, T.B., Wekerle, H., et al. (2009). Effector T cell interactions with meningeal vascular structures in nascent autoimmune CNS lesions. Nature *462*, 94–98.

De Bellis, M., Pisani, F., Mola, M.G., Basco, D., Catalano, F., Nicchia, G.P., Svelto, M., and Frigeri, A. (2014). A novel human aquaporin-4 splice variant exhibits a dominant-negative activity: a new mechanism to regulate water permeability. Mol. Biol. Cell *25*, 470–480.

Bennouna, S., Bliss, S.K., Curiel, T.J., and Denkers, Y. (2003). Cross-Talk in the Innate Immune System: Neutrophils Instruct Recruitment and Activation of Dendritic Cells during Microbial Infection.

Bradl, M., Misu, T., Takahashi, T., Watanabe, M., Mader, S., Reindl, M., Adzemovic, M., Bauer, J., Berger, T., Fujihara, K., et al. (2009). Neuromyelitis optica: pathogenicity of patient immunoglobulin in vivo. Ann. Neurol. *66*, 630–643.

Brück, W., Popescu, B., Lucchinetti, C.F., Markovic-Plese, S., Gold, R., Thal, D.R., and Metz, I. (2012). Neuromyelitis optica lesions may inform multiple sclerosis heterogeneity debate. Ann. Neurol. *72*, 385–394.

Cantrell, B.Y.D.A., and Smith, K.A. (1983). TRANSIENT EXPRESSION OF INTERLEUKIN C o n s e q u e n c e s for T Cell G r o w t h * 2 RECEPTORS Recent studies have revealed that T cell proliferation , although initiated by antigen or lectin , is actually mediated by a lymphocytotrophic hormone desig- . *158*, 1895–1911.

Crane, J.M., Lam, C., Rossi, A., Gupta, T., Bennett, J.L., and Verkman, a S. (2011). Binding affinity and specificity of neuromyelitis optica autoantibodies to aquaporin-4 M1/M23 isoforms and orthogonal arrays. J. Biol. Chem. *286*, 16516–16524.

Demetri, G.D., and Griffin, J.D. (1991). Granulocyte colony-stimulating factor and its receptor. Blood *78*, 2791–2808.

Fujihara, K., Misu, T., Nakashima, I., Takahashi, T., Bradl, M., Lassmann, H., Takano, R., Nishiyama, S., Takai, Y., Suzuki, C., et al. (2012). Neuromyelitis optica should be classified as an astrocytopathic disease rather than a demyelinating disease. Clin. Exp. Neuroimmunol. *3*, 58–73.

Graber, D.J., Levy, M., Kerr, D., and Wade, W.F. (2008). Neuromyelitis optica pathogenesis and aquaporin 4. J. Neuroinflammation *5*, 22.

Hinson SR1, Pittock SJ, Lucchinetti CF, Roemer SF, Fryer JP, Kryzer TJ, L.V. (2007). Pathogenic potential of IgG binding to water channel extracellular domain in neuromyelitis optica. Neurology.

Ishizu, T., Osoegawa, M., Mei, F.-J., Kikuchi, H., Tanaka, M., Takakura, Y., Minohara, M., Murai, H., Mihara, F., Taniwaki, T., et al. (2005). Intrathecal activation of the IL-17/IL-8 axis in opticospinal multiple sclerosis. Brain *128*, 988–1002.

Jacob, A., Matiello, M., Wingerchuk, D.M., Lucchinetti, C.F., Pittock, S.J., and Weinshenker, B.G. (2007). Neuromyelitis optica: changing concepts. J. Neuroimmunol. *187*, 126–138.

Jacob, A., Saadoun, S., Kitley, J., Leite, M., Palace, J., Schon, F., and Papadopoulos, M.C. (2012). Detrimental role of granulocyte-colony stimulating factor in neuromyelitis optica: clinical case and histological evidence. Mult. Scler. *18*, 1801–1803.

Jacob, A., McKeon, A., Nakashima, I., Sato, D.K., Elsone, L., Fujihara, K., and de Seze, J. (2013). Current concept of neuromyelitis optica (NMO) and NMO spectrum disorders. J. Neurol. Neurosurg. Psychiatry *84*, 922–930.

Jarius, S., and Wildemann, B. (2013). Aquaporin-4 antibodies (NMO-IgG) as a serological marker of neuromyelitis optica: a critical review of the literature. Brain Pathol. *23*, 661–683.

Jarius, S., Paul, F., Franciotta, D., Waters, P., Zipp, F., Hohlfeld, R., Vincent, A., and Wildemann, B. (2008). Mechanisms of disease: aquaporin-4 antibodies in neuromyelitis optica. Nat. Clin. Pract. Neurol. *4*, 202–214.

Johnson, J.L., Moore, E.E., Hiester, A.A., Tamura, D.Y., Zallen, G., and Silliman, C.C. (1999). Disparities in the respiratory burst between human and rat neutrophils Abstract: The

importance of reactive oxygen spe- cies (ROS) in neutrophil (PMN) -mediated injury to Oxygen consumption. *65*, 211–216.

Karussis, D. (2014). The diagnosis of multiple sclerosis and the various related demyelinating syndromes: A critical review. J. Autoimmun.

Kawakami, N., Lassmann, S., Li, Z., Odoardi, F., Ritter, T., Ziemssen, T., Klinkert, W.E.F., Ellwart, J.W., Bradl, M., Krivacic, K., et al. (2004). The activation status of neuroantigen-specific T cells in the target organ determines the clinical outcome of autoimmune encephalomyelitis. J. Exp. Med. *199*, 185–197.

Ketelslegers, I. a, Modderman, P.W., Vennegoor, A., Killestein, J., Hamann, D., and Hintzen, R.Q. (2011). Antibodies against aquaporin-4 in neuromyelitis optica: distinction between recurrent and monophasic patients. Mult. Scler. *17*, 1527–1530.

Kinoshita, M., Nakatsuji, Y., Kimura, T., Moriya, M., Takata, K., Okuno, T., Kumanogoh, A., Kajiyama, K., Yoshikawa, H., and Sakoda, S. (2009). Neuromyelitis optica: Passive transfer to rats by human immunoglobulin. Biochem. Biophys. Res. Commun. *386*, 623–627.

Kinoshita, M., Nakatsuji, Y., Kimura, T., Moriya, M., Takata, K., Okuno, T., Kumanogoh, A., Kajiyama, K., Yoshikawa, H., and Sakoda, S. (2010). Anti-aquaporin-4 antibody induces astrocytic cytotoxicity in the absence of CNS antigen-specific T cells. Biochem. Biophys. Res. Commun. *394*, 205–210.

Kira, J. (2003). Review Multiple sclerosis in the Japanese population Epidemiology of MS in Asia. *2*, 117–127.

Landis, D.M., and Reese, T.S. (1974). Arrays of particles in freeze-fractured astrocytic membranes. J. Cell Biol. *60*, 316–320.

Lennon, V. a, Kryzer, T.J., Pittock, S.J., Verkman, a S., and Hinson, S.R. (2005). IgG marker of optic-spinal multiple sclerosis binds to the aquaporin-4 water channel. J. Exp. Med. *202*, 473–477.

Levy, M., Wildemann, B., Jarius, S., Orellano, B., Sasidharan, S., Weber, M.S., and Stuve, O. (2014). Immunopathogenesis of neuromyelitis optica. Adv. Immunol. *121*, 213–242.

Litinskiy, M.B., Nardelli, B., Hilbert, D.M., He, B., Schaffer, A., Casali, P., and Cerutti, A. (2002). DCs induce CD40-independent immunoglobulin class switching through BLyS and APRIL. Nat. Immunol. *3*, 822–829.

Lucchinetti, C.F., Mandler, R.N., Mcgavern, D., Bruck, W., Gleich, G., Ransohoff, R.M., Trebst, C., Weinshenker, B., Wingerchuk, D., Parisi, J.E., et al. (2002). A role for humoral mechanisms in the pathogenesis of Devic ' s neuromyelitis optica. 1450–1461.

Matsushita, T., Matsuoka, T., Isobe, N., Kawano, Y., Minohara, M., Shi, N., Nishimura, Y., Ochi, H., and Kira, J. (2009). Association of the HLA-DPB1*0501 allele with anti-aquaporin-4

antibody positivity in Japanese patients with idiopathic central nervous system demyelinating disorders. Tissue Antigens *73*, 171–176.

McColl, S., and Staykova, MA, Staykova MA, Wozniak A, Fordham S, Bruce J, W. DO (1998). Treatment with anti-granulocyte antibodies inhibits the effector phase of experimental autoimmune encephalomyelitis. J. ….

Misu, T., Fujihara, K., Nakashima, I., Miyazawa, I., Okita, N., Takase, S., and Itoyama, Y. (2002). Pure optic-spinal form of multiple sclerosis in Japan. Brain *125*, 2460–2468.

Misu, T., Fujihara, K., Kakita, a, Konno, H., Nakamura, M., Watanabe, S., Takahashi, T., Nakashima, I., Takahashi, H., and Itoyama, Y. (2007a). Loss of aquaporin 4 in lesions of neuromyelitis optica: distinction from multiple sclerosis. Brain *130*, 1224–1234.

Misu, T., Fujihara, K., Kakita, a, Konno, H., Nakamura, M., Watanabe, S., Takahashi, T., Nakashima, I., Takahashi, H., and Itoyama, Y. (2007b). Loss of aquaporin 4 in lesions of neuromyelitis optica: distinction from multiple sclerosis. Brain *130*, 1224–1234.

Misu, T., Höftberger, R., Fujihara, K., Wimmer, I., Takai, Y., Nishiyama, S., Nakashima, I., Konno, H., Bradl, M., Garzuly, F., et al. (2013). Presence of six different lesion types suggests diverse mechanisms of tissue injury in neuromyelitis optica. Acta Neuropathol. *125*, 815–827.

Mitsdoerffer, M., Kuchroo, V., and Korn, T. (2013). Immunology of neuromyelitis optica: a T cell-B cell collaboration. Ann. N. Y. Acad. Sci. *1283*, 57–66.

Miyamoto, M., Prause, O., Sjöstrand, M., Laan, M., Lötvall, J., and Lindén, A. (2003). Endogenous IL-17 as a mediator of neutrophil recruitment caused by endotoxin exposure in mouse airways. J. Immunol. *170*, 4665–4672.

Moe, S.E., Sorbo, J.G., Sogaard, R., Zeuthen, T., Petter Ottersen, O., and Holen, T. (2008). New isoforms of rat Aquaporin-4. Genomics *91*, 367–377.

Nandhagopal, R., Al-Asmi, A., and Gujjar, A.R. (2010). Neuromyelitis optica: an overview. Postgrad. Med. J. *86*, 153–159.

Nathan, C. (2006). Neutrophils and immunity: challenges and opportunities. Nat. Rev. Immunol. *6*, 173–182.

Paxinos G, W.C. (1997). The rat brain in stereotaxic coor- dinates, 3rd edn (San Diego: Academic Press).

Pisani, F., Mastrototaro, M., Rossi, A., Nicchia, G.P., Tortorella, C., Ruggieri, M., Trojano, M., Frigeri, A., and Svelto, M. (2011). Identification of two major conformational aquaporin-4 epitopes for neuromyelitis optica autoantibody binding. J. Biol. Chem. *286*, 9216–9224.

Pittock, S.J., Lennon, V. a, de Seze, J., Vermersch, P., Homburger, H. a, Wingerchuk, D.M., Lucchinetti, C.F., Zéphir, H., Moder, K., and Weinshenker, B.G. (2008). Neuromyelitis optica and non organ-specific autoimmunity. Arch. Neurol. *65*, 78–83.

Pohl, M., Fischer, M.-T., Mader, S., Schanda, K., Kitic, M., Sharma, R., Wimmer, I., Misu, T., Fujihara, K., Reindl, M., et al. (2011). Pathogenic T cell responses against aquaporin 4. Acta Neuropathol. *122*, 21–34.

Pohl, M., Kawakami, N., Kitic, M., Bauer, J., Martins, R., Fischer, M.-T., Machado-Santos, J., Mader, S., Ellwart, J.W., Misu, T., et al. (2013). T cell-activation in neuromyelitis optica lesions plays a role in their formation. Acta Neuropathol. Commun. *1*, 85.

Rash, J.E., Yasumura, T., Hudson, C.S., Agre, P., and Nielsen, S. (1998). Direct immunogold labeling of aquaporin-4 in square arrays of astrocyte and ependymocyte plasma membranes in rat brain and spinal cord. Proc. Natl. Acad. Sci. U. S. A. *95*, 11981–11986.

Ratelade, J., and Verkman, a S. (2012). Neuromyelitis optica: aquaporin-4 based pathogenesis mechanisms and new therapies. Int. J. Biochem. Cell Biol. *44*, 1519–1530.

Ratelade, J., Bennett, J., and Verkman, A. (2011a). Evidence against cellular internalization in vivo of NMO-IgG, aquaporin-4, and excitatory amino acid transporter 2 in neuromyelitis optica. J. Biol. Chem.

Ratelade, J., Bennett, J.L., and Verkman, a S. (2011b). Intravenous neuromyelitis optica autoantibody in mice targets aquaporin-4 in peripheral organs and area postrema. PLoS One *6*, e27412.

Ratelade, J., Zhang, H., Saadoun, S., Bennett, J.L., Papadopoulos, M.C., and Verkman, a S. (2012). Neuromyelitis optica IgG and natural killer cells produce NMO lesions in mice without myelin loss. Acta Neuropathol. *123*, 861–872.

Rice, C.M., Cottrell, D., Wilkins, A., and Scolding, N.J. (2013). Primary progressive multiple sclerosis: progress and challenges. J. Neurol. Neurosurg. Psychiatry *84*, 1100–1106.

Rossi, A., Crane, J.M., and Verkman, a S. (2011). Aquaporin-4 Mz isoform: brain expression, supramolecular assembly and neuromyelitis optica antibody binding. Glia *59*, 1056–1063.

Saadoun, S., Waters, P., Bell, B.A., Vincent, A., Verkman, a S., and Papadopoulos, M.C. (2010). Intra-cerebral injection of neuromyelitis optica immunoglobulin G and human complement produces neuromyelitis optica lesions in mice. Brain *133*, 349–361.

Saadoun, Samira, Bridges Leslie, Verkman A.S., M.C.P. (2013). Paucity of natural killer and cytotoxic T cells in human neuromyelitis optica lesions. *23*, 1044–1047.

Segal, A.W. (2007). Europe PMC Funders Group How Neutrophils Kill Microbes. *2*.

Stavnezer, J. Immunoglobulin class switching Cytokines direct switching by regulating germline transcription. 199–205.

Uzawa, A., Mori, M., Arai, K., Sato, Y., Hayakawa, S., Masuda, S., Taniguchi, J., and Kuwabara, S. (2010). Cytokine and chemokine profiles in neuromyelitis optica: significance of interleukin-6. Mult. Scler. *16*, 1443–1452.

Varrin-Doyer, M., Spencer, C.M., Schulze-Topphoff, U., Nelson, P. a, Stroud, R.M., Cree, B. a C., and Zamvil, S.S. (2012). Aquaporin 4-specific T cells in neuromyelitis optica exhibit a Th17 bias and recognize Clostridium ABC transporter. Ann. Neurol. *72*, 53–64.

Verbavatz, J.M., Ma, T., Gobin, R., and Verkman, a S. (1997). Absence of orthogonal arrays in kidney, brain and muscle from transgenic knockout mice lacking water channel aquaporin-4. J. Cell Sci. *110 (Pt 2*, 2855–2860.

Vincent, A., Verkman, A.S., and Marios, C. (2013). NIH Public Access. *71*, 323–333.

Vincent, T., Saikali, P., Cayrol, R., Roth, A.D., Bar-Or, A., Prat, A., and Antel, J.P. (2008). Functional consequences of neuromyelitis optica-IgG astrocyte interactions on blood-brain barrier permeability and granulocyte recruitment. J. Immunol. *181*, 5730–5737.

Warabi, Y., Yagi, K., Hayashi, H., and Matsumoto, Y. (2006). Characterization of the T cell receptor repertoire in the Japanese neuromyelitis optica: T cell activity is up-regulated compared to multiple sclerosis. J. Neurol. Sci. *249*, 145–152.

Wauben, M.H., van der Kraan, M., Grosfeld-Stulemeyer, M.C., and Joosten, I. (1997). Definition of an extended MHC class II-peptide binding motif for the autoimmune disease-associated Lewis rat RT1.BL molecule. Int. Immunol. *9*, 281–290.

Wingerchuk, D.M. (2007). Neuromyelitis optica: new findings on pathogenesis. Int. Rev. Neurobiol. *79*, 665–688.

Wingerchuk, D.M., Lennon, V. a, Pittock, S.J., Lucchinetti, C.F., and Weinshenker, B.G. (2006a). Revised diagnostic criteria for neuromyelitis optica. Neurology *66*, 1485–1489.

Wingerchuk, D.M., Hogancamp, W.F., Brien, P.C.O., Brian, G., Frcp, C., and Weinshenker, B.G. (2006b). The clinical course of neuromyelitis optica (Devic ' s syndrome).

Wingerchuk, D.M., Lennon, V. a, Lucchinetti, C.F., Pittock, S.J., and Weinshenker, B.G. (2007). The spectrum of neuromyelitis optica. Lancet Neurol. *6*, 805–815.

Yukutake, Y., and Yasui, M. (2010). Regulation of water permeability through aquaporin-4. Neuroscience *168*, 885–891.

10. Supplementary Data

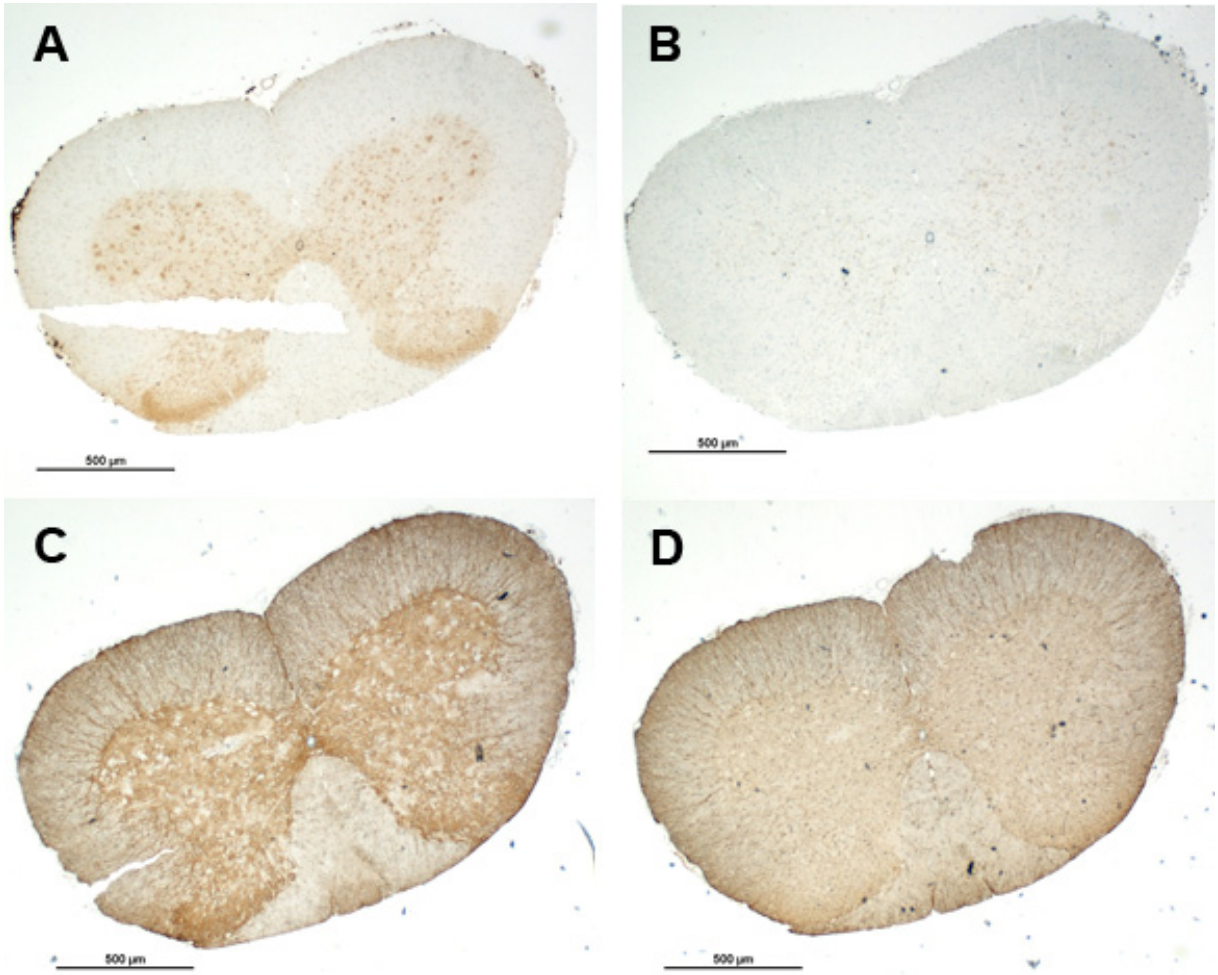

Supplementary Figure 1: Cervical spinal cord lesion causes by $AQP4_{207-232}$-specific T-cells. CD-3 staining of T-cells. T-cells are caught in the meninges, no infiltrating T-cells are observed (A). ED-1 staning of macrophages. No macrophages are recruited to this lesion site (B). AQP4 staining of spinal cord tissue. No AQP4-loss observed (C). GFAP staining of astrocytes. We do not observe GFAP loss, therefore no astrocyte damage is caused (D).

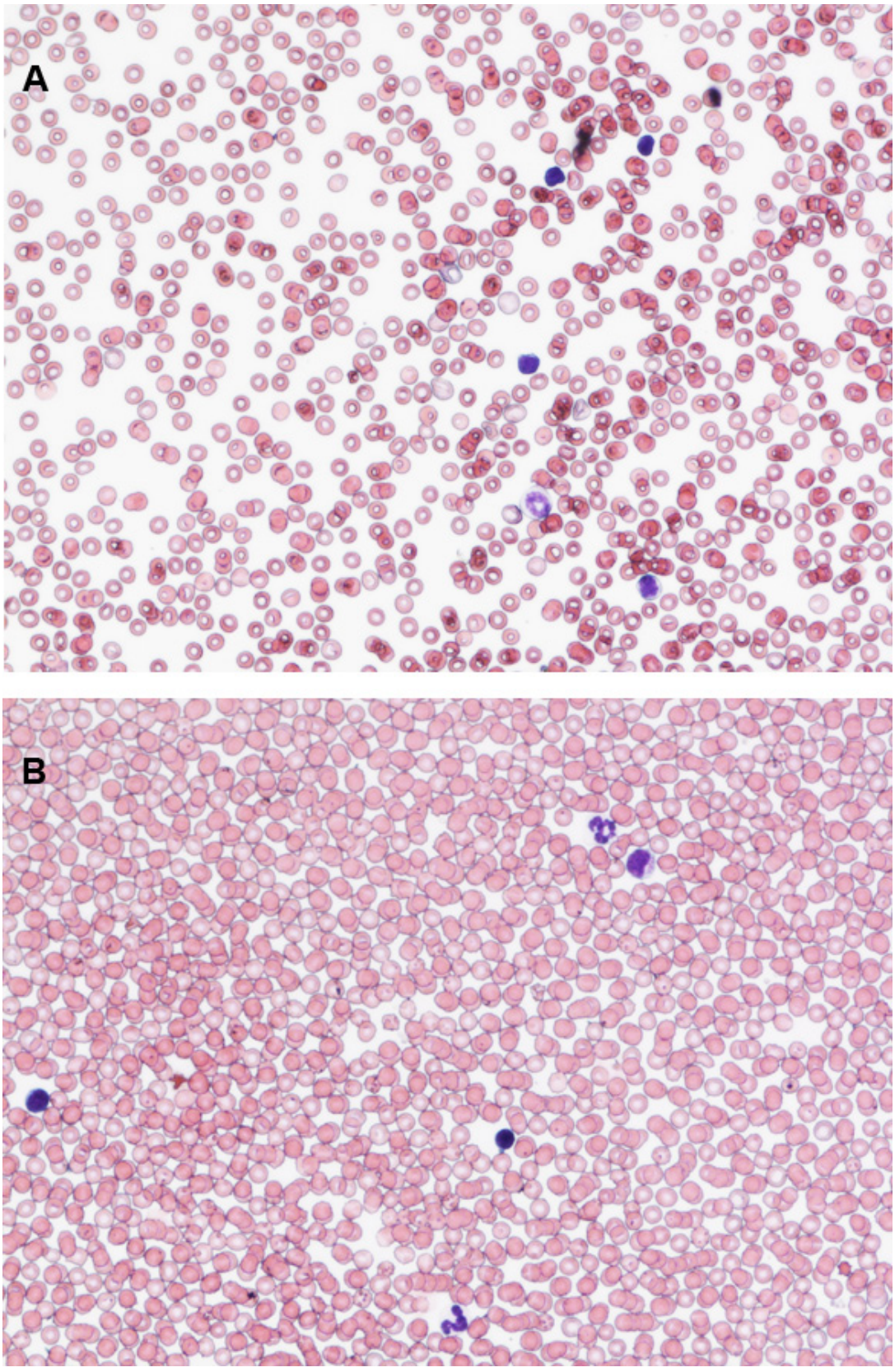

Supplementary Figure 2: Blood-smear of Lewis rats which were treated with PBS (A) or G-CSF by subcutaneous administration. Taken at a 25 x magnification.

11. Curriculum Vitae

Personal Data

Name	Bleranda Zeka

Education

09/1996 – 06/2000	Primary School, Grubergasse
09/2000 – 06/2008	Secondary School, BRG 16 Schuhmeierplatz
10/2008 – 05/2012	Bachelor: Biology at the University of Vienna, focus on Molecular Biology
10/2012 – 04/2012	Master: Molecular Biology at the University of Vienna, focus on Neuroscience

Laboratory experience

07/2011 – 08/2011	Bachelor's Thesis at University of Vienna, Department for Cell Biology and Biochemistry, group Wiche. Analysis of cytosketal proteins in Plectin-deficient cells
02/2013	Practical Course, "Wahlbeispiel" at Center for Brain Research, Medical University of Vienna, group Scholze. Isolation of an antibody against the alpha 5 nicotinic receptor subunit.
12/2012 – 01/2013	Practical Course at the University of Vienna, Department for Molecular Evolution, David Fredman. Analysis of Core Promoter Structure
09/2013 – 04/2014	Master's Thesis at Medical University of Vienna, Center for Brain Research, group

	Bradl. Pathogenicity of AQP4207-232 specific T-cells and the contribution of neutrophils to lesion formation

Computer Skills

Programming	Perl – good knowledge
	R – good knowledge
	Python – basic knowledge
	C - basic knowledge
Web	HTML
	CSS
Programs	Adobe Photoshop and Illustrator
	Linux Bash
	Microsoft Office

Language

	German – fluently
	English – fluently
	French – basic knowledge
	Albanian – native speaker

Awards

01/2014	Performance Scholarship, University of Vienna